

1 **Distinct phases of natural landscape dynamics and intensifying human activity**  
2 **in the central Kenya Rift Valley during the past 1300 years**

3 **Running head:** Past human influence on a Kenya Rift Valley landscape

4 Geert W. van der Plas<sup>1</sup>, Gijs De Cort<sup>1,2</sup>, Nik Petek-Sargeant<sup>3</sup>, Tabitha Wuytack<sup>1</sup>, Daniele  
5 Colombaroli<sup>1\*</sup>, Paul J. Lane<sup>4,5</sup> and Dirk Verschuren<sup>1</sup>

6 <sup>1</sup>*Limnology Unit, Department of Biology, Ghent University, K.L. Ledeganckstraat 35, B-9000*  
7 *Gent, Belgium*

8 <sup>2</sup>*Department of Earth Sciences, Royal Museum for Central Africa, B-3080 Tervuren, Belgium*

9 <sup>3</sup>*Department of Africa, Oceania and the Americas, The British Museum, Great Russell Street,*  
10 *London WC1B 3DG, UK*

11 <sup>4</sup>*Department of Archaeology, University of Cambridge, Downing Street, Cambridge, CB2 3DZ,*  
12 *UK*

13 <sup>5</sup>*Department of Archaeology & Ancient History, Uppsala University, S-752 36 Uppsala, Sweden*

14 *\*Present address: Centre for Quaternary Research, Department of Geography, Royal Holloway,*  
15 *University of London, Egham, Surrey TW20 0EX, UK*

16 **Correspondence:** Geert van der Plas (tel: +32-9-264-8792, e-mail: geert.vanderplas@ugent.be);  
17 Dirk Verschuren (tel: +32-9-264-5262, e-mail: dirk.verschuren@ugent.be)

18 **Abstract**

19 Socio-ecological stresses currently affecting the semi-arid regions of equatorial East Africa are  
20 driving environmental changes that need to be placed in a proper context of long-term human-  
21 climate-landscape interaction. Here we present a detailed reconstruction of past human influences

22 on the landscape of the central Kenya Rift Valley, against the backdrop of natural climate-driven  
23 ecosystem dynamics over the past 1300 years. Proxy records of vegetation dynamics (pollen),  
24 animal husbandry (fungal spores), biomass burning (charcoal) and soil mobilization (clastic  
25 mineral influx) extracted from the continuous depositional archive of Lake Bogoria reveal six  
26 distinct phases of human activity. From *ca* 700 to 1430 CE, strong primary response of savanna  
27 woodland ecotonal vegetation to climatic moisture-balance variation suggests that anthropogenic  
28 influence on regional ecosystem dynamics was limited. The first unambiguous ecological  
29 signature of human activities involves a mid-15<sup>th</sup> century reduction of woodland/forest trees  
30 followed by the appearance of cereal pollen, both evidence for mixed farming. From the mid-17<sup>th</sup>  
31 century, animal husbandry became a significant ecological factor and reached near-modern levels  
32 by the mid-19<sup>th</sup> century, after severe early-19<sup>th</sup> century drought had substantially changed human-  
33 landscape interaction. A short-lived peak in biomass burning and evidence for soil mobilization  
34 in low-lying areas of the Bogoria catchment likely reflects the known 19<sup>th</sup>-century establishment  
35 of irrigation agriculture, while renewed expansion of forest and woodland trees reflect the return  
36 of a wetter climate and abandonment of other farmland. Since the mid-20<sup>th</sup> century, the principal  
37 signature of human activity within the Lake Bogoria catchment is the unprecedented increase in  
38 clastic sediment flux, reflecting widespread soil erosion associated with rapidly intensifying land  
39 use.

40 **Keywords:** Anthropocene, climate-human interaction, disturbance ecology, East Africa, Kenya  
41 Rift Valley, Lake Bogoria, landscape ecology, paleoecology, vegetation dynamics

42 **Paper type:** Primary research

43 **1. Introduction**

44 The ever-increasing influence of human activity on virtually all aspects of the natural world has  
45 underlined the need for better understanding of longer-term climate-human-ecosystem  
46 interaction, knowledge that is essential for the sound and sustainable management of cultural  
47 landscapes. Establishing this long-term historical context is especially problematic in Africa,  
48 where hominin influence on the environment, through use of tools and fire, may even predate the  
49 origin of modern humans as biological species ~300,000 years ago (Gowlett, 2016; Schlebusch et  
50 al., 2017). Many authors suggest that human influence on the East African landscape must have  
51 become substantial with the introduction of food production (e.g. Taylor, 1990; Jolly et al., 1997;  
52 Heckmann et al., 2014). But, while archaeological evidence indicates that crop agriculture has  
53 been practiced in eastern equatorial Africa for roughly 2500 years (Fuller & Hildebrand, 2013;  
54 Lane, 2015), paleoecological signatures for marked landscape transformation have so far mostly  
55 been documented only from a few small regions where suitable natural archives, such as lake and  
56 bog deposits, can be found (Marchant et al., 2018). The combined evidence suggests that human  
57 impact visible in proxy records may have been limited to ‘niche’ environments or ‘islands’ within  
58 a mosaic landscape that offered early farmers a fortuitous combination of climate, topography,  
59 and soils (Marshall & Hildebrand, 2002; Widgren & Sutton, 2004), while people practicing  
60 nomadic or transhumant lifestyles exerted a relatively light footprint on the region’s savanna  
61 environments (Lane, 2016). Some studies of ancient land-use patterns in tropical Africa, based on  
62 extrapolation from historical population trends (e.g. Ramankutty & Foley, 1999; Houghton &  
63 Hackler, 2006) even suggest that disruptive human impacts on East Africa’s ecosystems must  
64 have been very limited prior to two-three centuries ago, due to the very low demographic  
65 pressure of its ancient inhabitants compared to their present-day counterparts. Substantial  
66 differences exist between various reconstructions (e.g., Kaplan et al., 2011; Klein Goldewijk et  
67 al., 2011) of the spatial extent of land areas subject to farming and grazing prior to

68 industrialization or the era of colonial governance. This situation translates into significant  
69 uncertainty about the magnitude of anthropogenic climate forcing attributable to (pre-) historical  
70 greenhouse-gas emissions (Stocker et al., 2018); and calls for improved documentation of land-  
71 use change during recent millennia worldwide (Harrison et al., 2018).

72 Documenting the long-term history of climate-human-landscape interaction in East Africa is  
73 complicated by the challenge of discriminating between the paleoecological signatures of human  
74 activities and the response of local vegetation ecotones and fire regimes to the variation in  
75 available moisture associated with natural climate variability (Colombaroli et al., 2014). A  
76 second challenge is the relative scarcity of paleoenvironmental archives with demonstrated  
77 continuity throughout the last few millennia, because large natural climate variability has  
78 repeatedly caused the (near-) desiccation of many lake and bog sites, and hence partial loss of  
79 their sedimentary archives, in the relatively recent past (Verschuren, 2003). Nevertheless,  
80 increased availability of continuous paleoclimate and paleohydrological records with high  
81 temporal resolution, and regional syntheses thereof (Verschuren, 2004; Verschuren & Charman,  
82 2008; Tierney et al., 2013; Nash et al., 2016), have greatly improved our insight into the  
83 spatiotemporal patterns of environmental change in East Africa at decadal to century timescales.  
84 These records can now be compared directly with the reconstructions of human activity.

85 This study aims to elucidate historical changes in the relative role of natural and anthropogenic  
86 processes in East Africa through a detailed paleoecological analysis of vegetation and landscape  
87 dynamics in the tropical semi-arid Rift Valley region of central Kenya over the last 1300 years.  
88 Multi-proxy data extracted from the sediment record of Lake Bogoria are set within a tight  
89 reference frame of the region's hydroclimatic history, as reconstructed from sedimentological and  
90 geochemical moisture-balance proxies in the same sediment record (De Cort et al., 2018). Further

91 we compare the paleoecological data with regional archaeological evidence, in order to assess  
92 discipline-specific perspectives on past landscape change (cf. Caseldine & Turney, 2010).  
93 Importantly, our proxy data represent continuous time series from *ca* 700 CE (*ca* 1250 calendar  
94 years BP) until the present (2014 CE). This allows for direct comparison of the relative  
95 magnitude of ancient landscape changes with those that occurred during the colonial period (i.e.,  
96 from *ca* 1900 CE) and after Kenya attained political independence in 1963. By quantifying those  
97 recent changes independently using historical data, issues of interpretation related to the  
98 sensitivity of proxies used to reconstruct the more ancient changes can be circumvented (cf.  
99 Dearing et al., 2006).

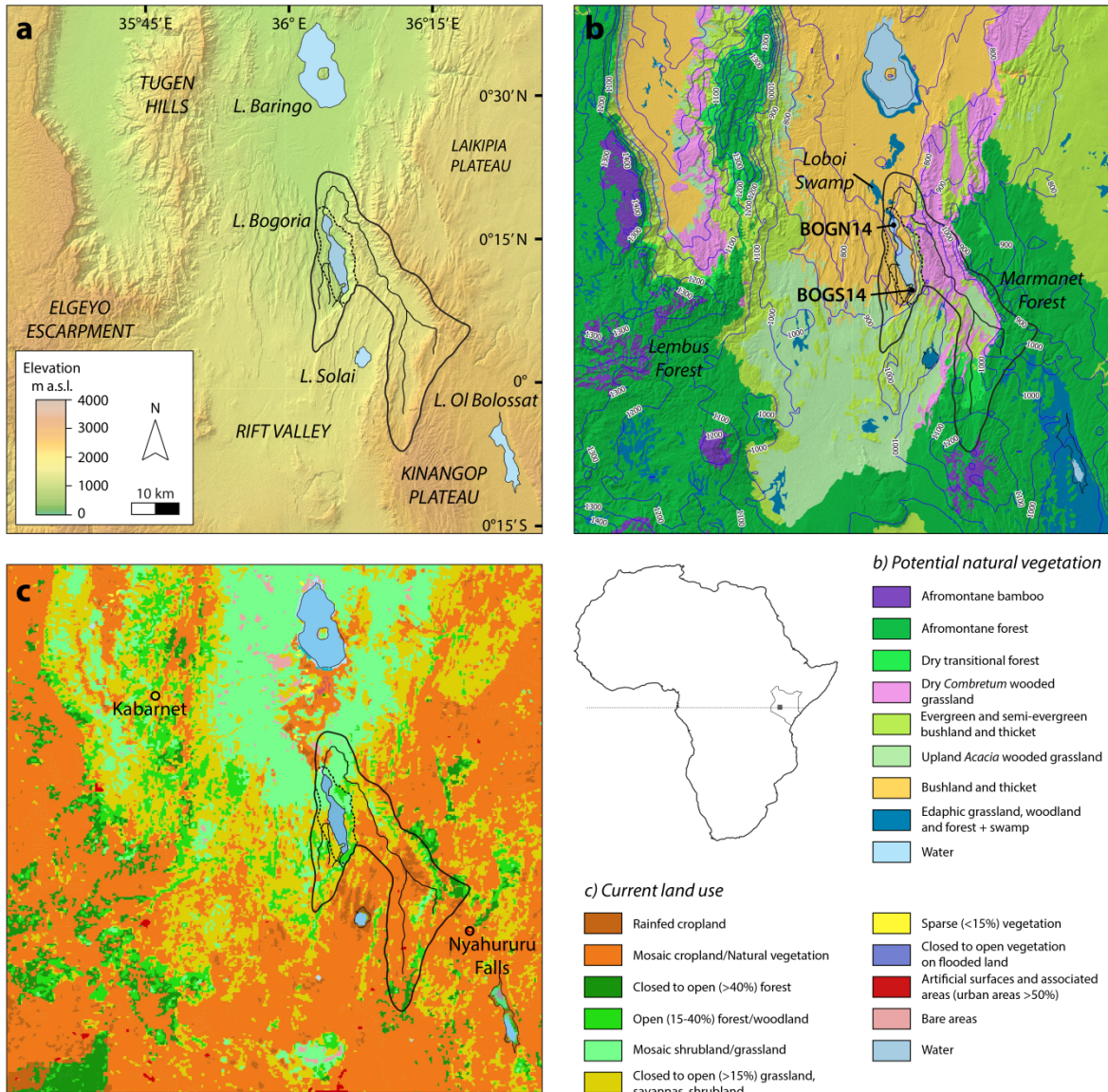
## 100 **2. Regional setting**

### 101 2.1 Geographical location, climate and hydrology

102 Lake Bogoria (0°15'N, 36°06'E; *ca* 17 x 3.5 km) is a hypersaline closed-basin lake occupying  
103 the southern end of a half-graben depression in the central Kenya Rift Valley (Fig. 1a). Its 705  
104 km<sup>2</sup> catchment is bounded to the east by the Laikipia Plateau. The Tugen Hills and Elgeyo  
105 Escarpment, which form the valley's western flank, are located *ca* 35 km to the west.

106 Rainfall seasonality in equatorial East Africa is linked to latitudinal migration of the tropical rain  
107 belt (Nicholson, 1996, 2018; Yang et al., 2015), which passes across the region twice each year  
108 and thus produces two rainy seasons: the long rains (March to May) and short rains (October and  
109 November). Both long and short rains are brought in from the Indian Ocean by, respectively,  
110 south-easterly and north-easterly monsoon winds. Located in the rain shadow of the eastern  
111 escarpment, Lake Bogoria's catchment receives rather little of this rainfall (500-1000 mm). This  
112 is however compensated by frequent late-afternoon cloud-bursts during the so-called dry season

113 (June to September), which deliver considerable amounts of precipitation from moist westerly air  
114 (Davies et al., 1985). Although its water budget is climate-controlled, geothermal springs fed by  
115 percolated rainwater provide the lake with 30-35% of its annual inflow and buffer the lake's  
116 surface level against short-term rainfall anomalies. Over longer time scales, this continuous  
117 geothermal inflow has also protected Lake Bogoria against complete desiccation during past  
118 episodes of severe climatic drought (Renaut & Tiercelin, 1994; Onyando et al., 2005). As a  
119 result, its bottom sediments have preserved a regionally unique continuous record of climate and  
120 landscape history throughout at least the last 1300 years (De Cort et al., 2013, 2018). Lake  
121 Bogoria is divided into three basins along its length, separated by sills that are currently  
122 submerged. About two-thirds of its catchment is drained by the Sandai-Waseges River, which  
123 enters the lake from the north via a broad floodplain. It is a mostly seasonal river, but can be  
124 perennial during exceptionally wet years (Renaut et al., 1986). In recent years water from the  
125 river has been diverted for crop irrigation immediately north of the lake. The narrow western and  
126 southern portions of the catchment are drained by small ephemeral streams which flow into the  
127 central and southern basins. The Lake Bogoria National Reserve (107 km<sup>2</sup>; Fig. 1a) protects the  
128 lake and immediately adjacent catchment areas from anthropogenic impact, but not the large  
129 upstream portions of the Sandai-Waseges drainage, which are thus more susceptible to  
130 disturbance.



131  
 132 **Fig. 1** (a) Location of Lake Bogoria, its drainage basin (bold line), major rivers feeding into the  
 133 lake (thin lines) and the Lake Bogoria National Reserve (boundary as stippled line), in relation to  
 134 other regional lakes and surrounding topography. Topography data are from the Advanced  
 135 Spaceborne Thermal Emission and Reflection Radiometer (ASTER) Global Digital Elevation  
 136 Model (GDEM) data set (NASA LP DAAC, 2011). (b) Potential vegetation of the study region,  
 137 simplified from the VECEA classification (van Breugel et al., 2015). Superimposed on this map  
 138 are the isolines of mean annual rainfall for the period 1970-2000 based on the Worldclim 2.0  
 139 dataset (Fick & Hijmans, 2017) shown to highlight the moisture dependence of vegetation  
 140 distribution. (c) Map of current land cover and land use, derived from Globcover data for 2009  
 141 (Bontemps, 2011) using a regional model by the Food and Agriculture Organization of the  
 142 United Nations (FAO, 2015). The skeleton map shows the location of the study area in eastern  
 143 equatorial Africa.

## 144 2.2 Modern-day vegetation

145 Modern-day vegetation around Lake Bogoria falls within the Somalia-Masai phytogeographic  
146 region as defined by White (1983). According to Vincens et al. (2006), vegetation in the direct  
147 vicinity of the lake can all be broadly classified under the biomes of tropical savanna and dry  
148 forest. At mid-elevations on the eastern escarpment these authors report the occurrence of *Acacia*  
149 wooded grassland with *Combretum*, *Tarchonanthus*, *Dodonaea* and *Justicia* as other principal  
150 arboreal taxa (i.e., trees) and Amaranthaceae as most common herbaceous taxa (i.e., herbs).  
151 Somewhat less open woodland occurs on the low ridge along on the west side of the lake with  
152 *Dodonaea* as the dominant tree species together with *Terminalia* and sparse thickets of *Acacia*  
153 *brevispica*, while south of the lake *Tarchonanthus* is the most abundant tree (Vincens et al.,  
154 2006). In the wider region of the central Rift Valley, wooded grassland dominated by *Combretum*  
155 and *Terminalia* tends to occur mostly on westward slopes, whereas evergreen bushland with  
156 *Dodonaea*, *Euphorbia*, *Olea* and *Tarchonanthus* occurs more on eastward slopes (Fig. 1b; Kindt  
157 et al., 2011b; Van Breugel et al., 2015). Closed-canopy Afromontane forest is mostly lacking  
158 within the Bogoria catchment (Fig.1c), and found only within Marmanet Forest in the southeast  
159 (Vincens et al., 1986) and in dry coniferous forest dominated by *Podocarpus*, *Juniperus*, *Olea*  
160 and *Dodonaea* in the south. Outside the Bogoria catchment, Afromontane forest is found above  
161 2000 m elevation in Lembus Forest near Kabarnet, *ca* 45 km west of the lake; and on the Laikipia  
162 Plateau, from *ca* 25 km to the east, where it consists mostly of *Juniperus*, *Olea* and *Croton*  
163 (Taylor et al., 2005). Dry transitional forest consisting of *Calodendrum*, *Croton*, *Euclea*, *Olea*  
164 and a mix of other Afromontane and savanna trees used to rise from the woodlands up dry  
165 escarpment slopes, but very little of this biome remains in Kenya today (Kindt et al., 2011a).  
166 Today *Dodonaea viscosa*, native to the area but with a tendency to encroach into disturbed

167 vegetation (Becker et al., 2016), is common throughout the region's grassland-forest ecotone.  
168 Timber plantations with pine (*Pinus patula* and *P. radiata*) and cypress (*Cupressus arizonica*, *C.*  
169 *torulosa*, *C. macrocarpa*, etc.), both introduced since the early 1900s, now replace part of the  
170 region's indigenous forests (Troup, 1932; Ofcansky, 1984; Kokwaro, 2015).

### 171 **3. Materials and methods**

#### 172 3.1 Sediment sampling and chronology

173 The sediment cores analyzed in this study were collected from the deepest points of the southern  
174 and northern basins of Lake Bogoria in 2014, using gravity- and piston-coring equipment.  
175 Overlapping core sections were assembled in two composite sediment sequences labelled  
176 BOGS14 and BOGN14 (Fig. 1b), through cross-correlation using visual lithostratigraphic  
177 markers and magnetic-susceptibility scanning data (De Cort et al., 2018). The chronology of  
178 Lake Bogoria's sediment record is based on 16  $^{14}\text{C}$ -dated levels, together with  $^{210}\text{Pb}$ -dating of  
179 recent sediments and a comprehensive set of tie points between the respective sediment  
180 sequences (De Cort et al., 2018). Radiocarbon dating targeted terrestrial plant material, mostly  
181 small grass-charcoal fragments, but also terrestrial seeds and charred wood. Tie points between  
182 cores were established using visual characteristics, charcoal counts and geochemical data. Age-  
183 depth modelling was performed using Bacon software in R (Blaauw & Christen, 2011), after  
184 calibrating the  $^{14}\text{C}$  ages with the IntCal13 calibration curve (Reimer et al., 2013). There is a  
185 sizable analytical error on individual  $^{14}\text{C}$  dates compared to the total time period covered by the  
186 record. Combined with wide calendar-age windows associated with  $^{14}\text{C}$  dates younger than 700  
187 years (Reimer et al., 2013), and short-term variation in the rate of sediment accumulation  
188 associated with lake-level fluctuations (Verschuren, 1999, 2001) this translates into relatively

189 high age uncertainty on all sediment intervals beyond the  $^{210}\text{Pb}$ -dated range (De Cort et al., 2018;  
 190 Supplementary Fig. S1). In turn, this places an unavoidable upper limit to dating precision in  
 191 natural paleoenvironmental archives of this type and time range, even when applying state-of-the-  
 192 art Bayesian age-modelling techniques (e.g., Blaauw et al., 2011). These age uncertainties (Table  
 193 1) must be taken into account when comparing the results of this study with paleoecological  
 194 evidence from other sites, or with independently constrained historical data. However, since our  
 195 proxy evidence for past landscape changes is drawn from the same sediment archive as the proxy  
 196 evidence for hydroclimate change (De Cort et al., 2018), temporal relationships between the  
 197 reported sedimentary signatures of the respective events are secure.

198 **Table 1** Sediment depth, weighted-mean modelled age and the lower and upper boundaries of  
 199 95% confidence envelopes (Min/Max Age) of pollen-zone boundaries in composite sequence  
 200 BOGS14 from the southern basin of Lake Bogoria, based on  $^{210}\text{Pb}$ - and  $^{14}\text{C}$ -dating by De Cort et  
 201 al. (2018).

|                            | Depth | Mean Age  | Min. Age  | Max. Age  |
|----------------------------|-------|-----------|-----------|-----------|
|                            | (cm)  | (year CE) | (year CE) | (year CE) |
| Top of record              | 0     | 2014.6    | 2014.6    | 2014.6    |
| BOGS-5/BOGS-6 transition   | 13.8  | 1965      | 1958      | 1973      |
| BOGS-4b/BOGS-5 transition  | 30.4  | 1910      | 1876      | 1935      |
| BOGS-4a/BOGS-4b transition | 66.5  | 1670      | 1586      | 1750      |
| BOGS-3/BOGS-4a transition  | 107.1 | 1430      | 1399      | 1472      |
| BOGS-2b/BOGS-3 transition  | 127.1 | 1330      | 1282      | 1373      |
| BOGS-2a/BOGS-2b transition | 148.1 | 1250      | 1199      | 1296      |
| BOGS-1/BOGS-2a transition  | 176.4 | 1175      | 1127      | 1216      |
| Base of record             | 300   | 686       | 623       | 767       |

202

203

204 3.2 Pollen and fungal-spore analysis

205 Pollen samples for vegetation reconstruction were prepared according to standard procedures  
206 (Faegri & Iversen, 1964; Moore et al., 1991; see Supplementary Information for details). The  
207 targeted minimum pollen sum was 400 pollen grains of terrestrial plants (BOGS14: range 225-  
208 872, mean 567; BOGN14: range 111-576, mean 429). This sum excludes pollen of aquatic plants,  
209 Cyperaceae (sedges, in this environment also mostly aquatic or riparian), and all non-pollen  
210 palynomorphs (NPPs) such as fern and fungal spores. It does include cultivated plants such as  
211 pine (*Pinus*), a prolific pollen producer (see Supplementary Information for further comment).  
212 Most Cupressaceae pollen encountered in this study probably derives from the native *Juniperus*  
213 *procera*, an important element in the Afromontane forest of central Kenya (Lamb et al., 2003).  
214 However, post-1900 CE samples must also contain introduced cypress (*Cupressus*) species.

215 Analysis of fungal spores focused on coprophilous fungi, i.e. fungi growing either obligately or  
216 facultatively on the excrements of large herbivores (Baker et al., 2013), and selected other taxa  
217 such as *Glomus*, cf. *Helminthosporium* and *Tetraploa*. However, all spores were counted to  
218 assess their overall abundance relative to vascular-plant pollen. We used atlases of African NPPs  
219 (van Geel et al., 2011; Gelorini et al., 2011) as main reference for fungal-spore identification.  
220 Among the fungal spores recovered, we considered only *Sordaria* and *Sporormiella* as obligate  
221 coprophiles (Gelorini et al., 2012; Baker et al., 2013); this record yielded no *Delitschia* or  
222 *Podospora*. *Cercophora*, *Chaetomium* and the widespread saprotrophic *Coniochaeta* are  
223 considered facultative coprophiles, and thus less persuasive as proxies for past animal husbandry.  
224 The percent abundance of individual fungal spore taxa is expressed relative to the terrestrial  
225 pollen sum.

226 Constrained incremental sum-of-squares cluster analysis (CONISS; Grimm, 1987) of the fossil  
227 pollen assemblages was used to delineate stratigraphic pollen zones. This zonation is based only  
228 on the terrestrial pollen sum. Since fungal spores are not part of the pollen sum they are treated as  
229 an independent environmental variable. Stratigraphic changes in pollen-assemblage composition  
230 were visualized using TILIA 2.0.41 (Grimm, 2015). Indirect gradient analysis was used to extract  
231 the underlying comprehensive changes in pollen-assemblage composition. As the overall  
232 variability in our pollen data fits a linear model rather than a unimodal model, PCA was preferred  
233 over DCA (DCA axis 1 < 2 SD; Ter Braak & Prentice, 1988). To estimate how much of the  
234 variance in the response variable (vegetation) can be explained by variation in fire regime,  
235 Redundancy Analysis (RDA; preferred above the unimodal response model CCA, cf. above) was  
236 performed on the pollen data, using charcoal accumulation rate (CHAR) as the explanatory  
237 variable (Davies & Tso, 1982; Ter Braak & Prentice, 1988). In this approach, only the first  
238 canonical axis is constrained, whereas the other axes remain unconstrained ('hybrid redundancy  
239 analysis'; Colombaroli et al., 2009). All gradient analyses were performed using Canoco 5 (Ter  
240 Braak, 1988).

### 241 3.3 Size classes of Poaceae pollen grains

242 The traditional method to distinguish Poaceae pollen derived from cereals (i.e., domesticated  
243 grasses) from wild-type grass pollen is that grains <37 µm are counted as wild type while grains  
244 >37 µm are counted as cereals (Andersen, 1979). Developed for tracing European and Middle  
245 Eastern cereals, this criterion does not necessarily apply to the pollen of indigenous African  
246 cereals and wild-type grasses (Bonnefille 1972). Moreover, preparation methods using potassium  
247 hydroxide and acetolysis, as well as mounting of the pollen residue in glycerol, can cause  
248 swelling of the pollen grains (Moore & Webb, 1978; Dickson, 1988). Pollen grains of *Zea mays*

249 (maize, corn) are normally discriminated by their very large size (>85  $\mu\text{m}$ ; Eubanks, 1997).  
250 However, ancient maize pollen grains are sometimes found to be smaller than modern grains (60–  
251 85  $\mu\text{m}$  instead of the modern 85–125  $\mu\text{m}$ ; Tsukada & Rowley, 1964). Following Colombaroli et  
252 al. (2018), we opted for a conservative approach and divided Poaceae pollen into three size  
253 categories. Grains <60  $\mu\text{m}$  are considered to be derived from wild-type grass, although  
254 significant overlap with the indigenous cereals finger millet (*Eleusine coracana*) and sorghum  
255 (*Sorghum bicolor*) cannot be excluded (Chaturvedi et al., 1994). Grains >85  $\mu\text{m}$  are all assumed  
256 to be *Z. mays*; and grains in the 60-85  $\mu\text{m}$  range are assumed to be disproportionately derived from  
257 indigenous cereals, as opposed to wild-type grasses. Another complication is that the probability  
258 of finding wild-type grass pollen grains large enough to be misclassified as cereal pollen  
259 increases in proportion to the percentage (%) of Poaceae in the total pollen sum. To control for  
260 this artefact, we calculated the fraction of 60-85  $\mu\text{m}$  Poaceae grains relative to the total Poaceae  
261 pollen abundance in each sampling interval, and compared the average 60-85  $\mu\text{m}$  fraction for  
262 each pollen zone with the record-wide mean value.



264 **Fig. 2** Stratigraphic distribution of selected pollen taxa (most, but not all >1% of the terrestrial  
265 pollen sum) in the BOGS14 sediment sequence from the southern basin of Lake Bogoria, in  
266 relation to sediment age (De Cort et al., 2018) and pollen-based stratigraphic zonation (CONISS;  
267 Grimm, 1987). Taxon abundance is presented as percentage (%) of the terrestrial pollen sum  
268 (black curves; 10x exaggeration in white), with taxa grouped per vegetation type and summary  
269 diagram on the left. Pollen from wetland taxa and fungal spores are expressed as percent of the  
270 terrestrial pollen sum but not included in it.

271

## 272 **4. Results**

### 273 4.1 Landscape history as recorded in the southern basin of Lake Bogoria

#### 274 4.1.1 Evidence from vascular-plant pollen

275 The 1300-year record of terrestrial vegetation dynamics revealed by sediment sequence BOGS14  
276 comprises six pollen zones as defined by CONISS (Fig. 2). A detailed description is provided in  
277 Supplementary Information; here we summarize the main trends. On the whole in pollen zone  
278 BOGS-1 (ca 700-1175 CE), the pollen assemblage indicates that much of the catchment was  
279 covered by a relatively open grassland-woodland ecotone, with stands of closed-canopy forest  
280 relatively nearby. The grass pollen fraction is relatively high, fluctuating around 50% with two  
281 short-lived declines around 960 and 1130 CE (Fig. 2). The Afromontane forest component is  
282 substantial (mean 30%) and dominated by *Podocarpus*, *Olea* and Cupressaceae (at this time, the  
283 native *Juniperus procera*). The woodland fraction (mean 16%) is relatively stable through time  
284 and consists primarily of *Acalypha* with smaller contributions from Combretaceae, *Dodonaea*,  
285 *Euphorbia* and *Acacia*. The herbaceous component is relatively modest (mean 6%). In zone  
286 BOGS-2 (ca 1175-1330 CE), grass and *Acalypha* pollen decrease to levels well below those in  
287 BOGS-1 during two multi-decadal episodes centered around 1220 and 1280 CE. During the first  
288 episode (sub-zone BOGS-2a) this is mainly compensated by an increase of the forest component

289 (mean 38%) carried in large part by *Olea*. During the second (sub-zone BOGS-2b) there are  
290 major increases in diverse trees and herbs associated with *Acacia* wooded grassland. In zone  
291 BOGS-3 (*ca* 1330-1430 CE), grass pollen percentages increase again to a mean value of 50%.  
292 Taxa associated with *Acacia* wooded grassland are reduced, largely compensated by re-expansion  
293 of *Acalypha* to a level approaching that of BOGS-1. The total woodland and forest fractions  
294 remain similar to those in BOGS-1 and BOGS-2b.

295 Pollen zone BOGS-4 (*ca* 1430-1910 CE) encompasses a *ca* 500-year period of Rift Valley  
296 history. Grass percentages mostly exceed 60% and reach peak values of *ca* 75% around 1710 CE  
297 and 1840 CE, but decrease to *ca* 50% at the top of this zone. In the forest component, *Olea*  
298 maintains the mean level of 20% it had in BOGS-3 only until *ca* 1500 CE, after which it drops to  
299 *ca* 10%. Simultaneously, Poaceae grains in the size range 60-85  $\mu\text{m}$  start appearing more or less  
300 continuously and in significant numbers. Overall, the woodland component is strongly reduced to  
301 a mean value of 6% between *ca* 1480 and 1870 CE, coincident with the period of low *Olea*  
302 abundances (Fig. 2). Cf. *Ricinus* (castor oil plant), only occasionally present before, appears more  
303 regularly from *ca* 1600 CE onwards (Fig. 2). A concentration of percent-abundance shifts around  
304 1670 CE divides this zone in two sub-zones (BOGS-4a and BOGS-4b). Among forest taxa cf.  
305 *Calodendrum* and *Hagenia* decrease to the benefit of *Artemisia*, while among the woodland taxa  
306 *Dodonaea* decrease to the benefit of *Justicia* and *Euphorbia*.

307 In zone BOGS-5 (*ca* 1910-1965 CE), which broadly encompasses the period of European  
308 colonial governance, Poaceae pollen decrease further to reach a low value of *ca* 30% around  
309 1960 CE. Trees of *Acacia* wooded grassland all increase, suggesting a recovery of the woodland  
310 component (range 8-17%). This woodland recovery is also reflected in marked increases of  
311 herbaceous taxa belonging to the Amaranthaceae and Asteraceae, cf. *Ricinus* and *Tribulus*, and

312 diverse rare taxa (< 1% of the pollen sum) such as cf. *Corchorus*, cf. *Hypoestes*, Loranthaceae  
313 and Malvaceae (Fig. 2). The Afromontane forest component expands only temporarily in the  
314 lower part of this zone, representing the early 20<sup>th</sup> century. Finally, in zone BOGS-6 (ca 1965 –  
315 2014 CE), which broadly encompasses the post-colonial period, the fraction of Poaceae pollen  
316 declines further to reach a record low value of 18% in the pollen assemblage representing  
317 modern-day vegetation. However, the now strong Afromontane (38-46%), woodland (14-25%)  
318 and herbaceous (9-16%) components mostly benefit from the unprecedented increases in  
319 Cupressaceae, now to be attributed largely to exotic cypress species planted for timber  
320 production; as well as *Dodonaea* and ruderal herbs such as *Plantago* and cf. *Ricinus*. Also the  
321 exotic *Pinus* makes a strong appearance. Only a single Poaceae grain >85 µm (maize) was  
322 recovered from BOGS-6, and none in the 60-85 µm range.

#### 323 4.1.2 Spores of coprophilous and other fungi

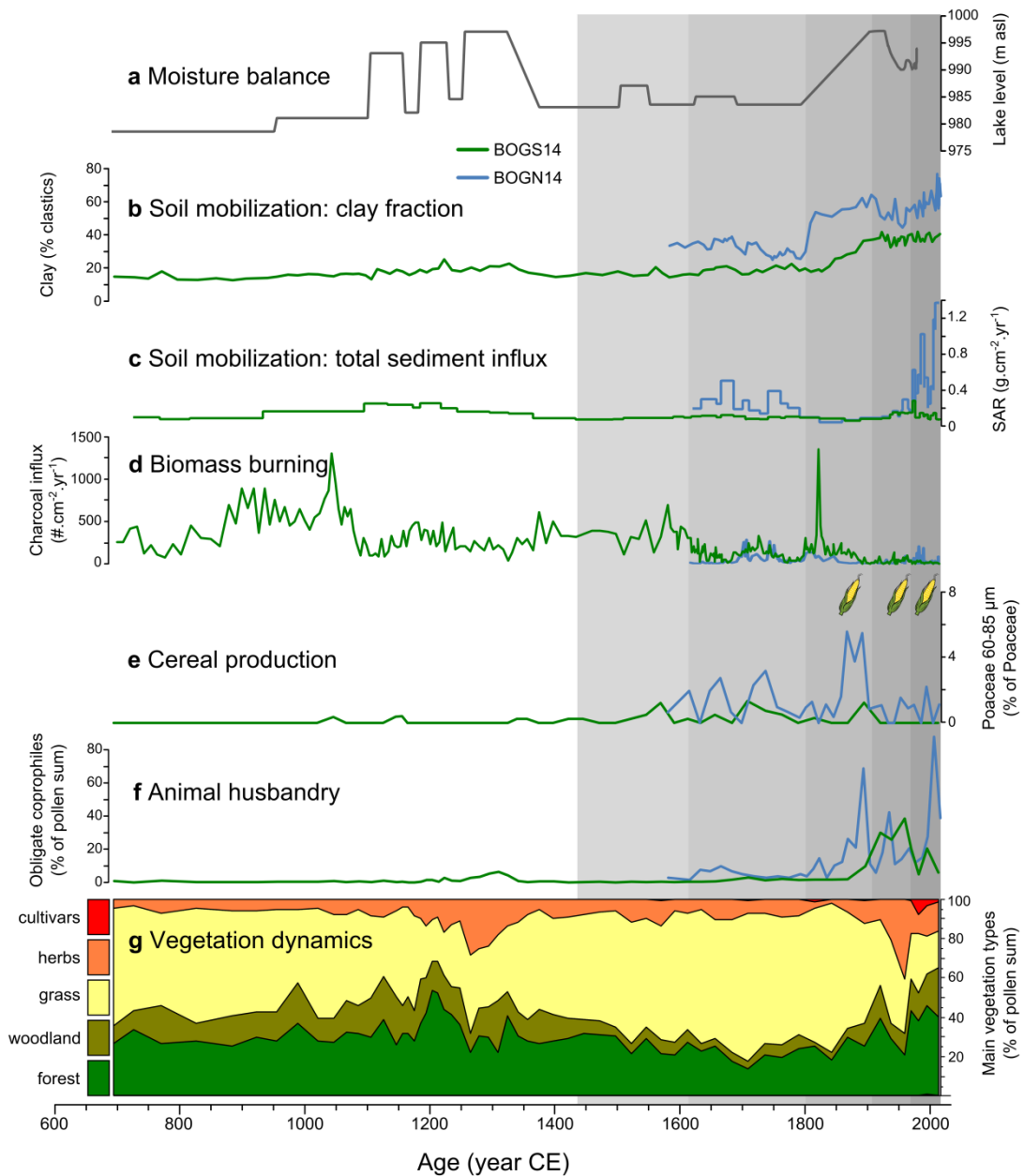
324 During the period 700–1175 CE (pollen zone BOGS-1) the most abundant fungal spores belong  
325 to cf. *Helminthosporium*, which occurs on grasses (Shoemaker, 1959); and *Coniochaeta*, a  
326 general saprotrophic taxon (Gelorini et al., 2011, 2012; Baker et al., 2013; Fig. 2). Also almost  
327 continuously present is *Tetraploa aristata*, a fungus found on the leaf bases and stems of living  
328 plants, including Poaceae and Cyperaceae (Ellis, 1971). The obligate coprophilous fungus  
329 *Sporormiella* and a few other taxa are present at very low abundances only. In BOGS-2  
330 *Sporormiella* is more common, especially during 1250–1330 CE. Also the obligate coprophile  
331 *Sordaria* is found, albeit in low percentages; and *Chaetomium*, a facultative coprophile. In  
332 BOGS-3 and BOGS-4a (ca 1330–1675 CE), fungal spore assemblages and abundances are  
333 similar to those recorded in BOGS-1. Starting from the base of BOGS-4b, *Sporormiella*  
334 abundances increase again to those attained in BOGS-2, and remain at that (overall still relatively

335 modest) level until near the top of BOGS-4b (Fig. 2). Early during this period there are also  
336 temporary peaks in cf. *Helminthosporium* and *Coniochaeta*, and brief appearances of  
337 *Chaetomium* and *Sordaria* but the two latter taxa disappear again shortly thereafter. From ca  
338 1890 CE until the 1960s (largely corresponding with BOGS-5) *Sporormiella* increase  
339 dramatically, together with modest but still significant increases in cf. *Helminthosporium*,  
340 *Coniochaeta* and *Tetraploa aristata*. In BOGS-6 (the last 50 years) the total abundance of fungal  
341 spores delivered to southern Lake Bogoria sediments is reduced, with notable decreases in  
342 *Sporormiella*, cf. *Helminthosporium* and *Coniochaeta*.

#### 343 4.1.3 Charcoal

344 The influx of charcoal to the southern basin of Lake Bogoria exhibits high temporal variability at  
345 the (sub-)decadal time scale during the past 1300 years (Fig. 3d). Initially, charcoal influx  
346 displays an inverse relationship with local hydroclimatic variability (Fig. 3a; De Cort et al.,  
347 2018). This is the case in pollen zones BOGS-1 through BOGS-3 (the period from ca 700 to 1430  
348 CE), with the exception of BOGS-1a when charcoal influx is low while climate conditions are  
349 inferred to have been dry. On average, the highest sustained charcoal influx in this ca 700-year  
350 period ( $>500$  particles  $\text{cm}^{-2}\text{yr}^{-1}$ ) occurred from ca 880 to 1070 CE, with a peak of 1300 particles  
351  $\text{cm}^{-2}\text{yr}^{-1}$  around 1040 CE. The lowest charcoal influx occurred in the second half of the 8<sup>th</sup>  
352 century CE ( $<250$  particles  $\text{cm}^{-2}\text{yr}^{-1}$ ) and around 1110 CE and 1320 CE ( $<100$  particles  $\text{cm}^{-2}\text{yr}^{-1}$ ).  
353 In BOGS-4a, fluctuating but mostly high charcoal influx values averaging 300-400 particles  $\text{cm}^{-2}\text{yr}^{-1}$   
354 are sustained throughout the 15<sup>th</sup> and 16<sup>th</sup> century. They reach a peak of  $>600$  particles  $\text{cm}^{-2}\text{yr}^{-1}$   
355 around 1580 CE before decreasing to very low levels ( $<100$  particles  $\text{cm}^{-2}\text{yr}^{-1}$ ) toward the  
356 top of BOGS-4a and the base of BOGS-4b, dated to the late 17<sup>th</sup> century CE. Charcoal influx  
357 remains very to moderately low (most often  $<200$  particles  $\text{cm}^{-2}\text{yr}^{-1}$ ) throughout the 18<sup>th</sup> and 19<sup>th</sup>

358 centuries, with the exception of a pronounced but short-lived maximum (1345 particles  $\text{cm}^{-2}\text{yr}^{-1}$ )  
 359 dated to *ca* 1820 CE, just after the start of a progressive rise in reconstructed lake level. At the  
 360 top of BOGS-4b, i.e. the turn of the 20<sup>th</sup> century, charcoal influx values reach an extreme low  
 361 point (5 particles  $\text{cm}^{-2}\text{yr}^{-1}$ ) after which they remain low (usually  $<100$  particles  $\text{cm}^{-2}\text{yr}^{-1}$ ) until the  
 362 present-day.



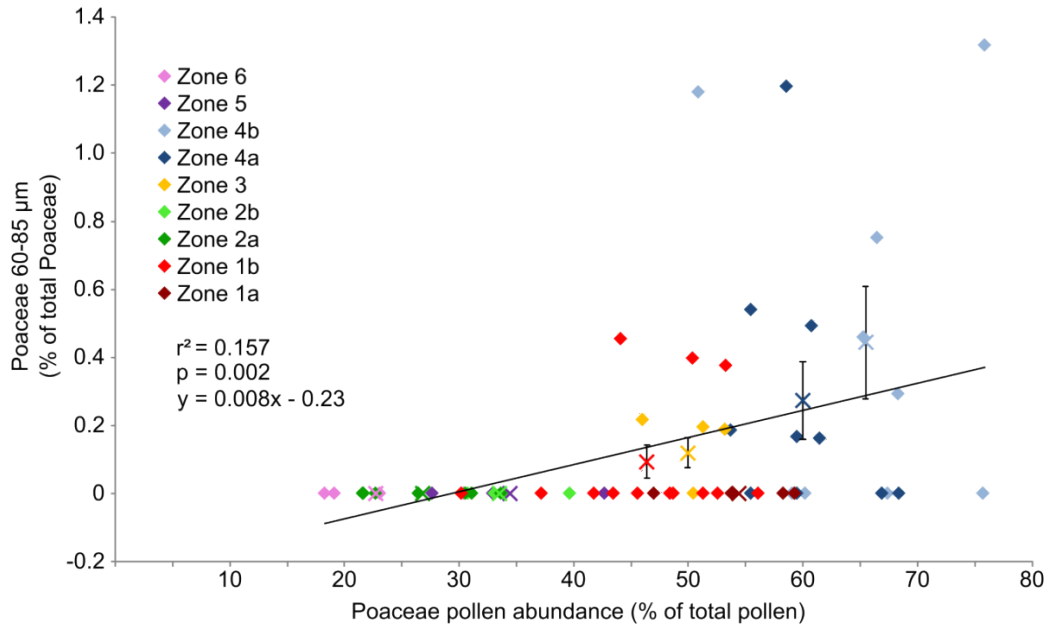
363

364 **Fig. 3** Synthesis of proxy data from the southern (BOGS14, green) and northern (BOGN14, blue)  
365 sediment record of Lake Bogoria, with indication of the five phases of intensifying ecological  
366 influence of human activity (light to dark grey shading). The panels show (a) climatic moisture-  
367 balance variation inferred from lake-level change, simplified from De Cort et al. (2018); (b) clay  
368 fraction as % of clastic mineral sediment; (c) total lake-sediment accumulation rate (SAR); (d)  
369 biomass burning inferred from charcoal influx; (e) cereal production inferred from the fraction of  
370 Poaceae pollen grains sized 60-85  $\mu\text{m}$ , with isolated finds of maize pollen (Poaceae grains  $>85$   
371  $\mu\text{m}$ ) indicated with pictograms; (f) Animal husbandry (plus wild herbivores; see text), inferred  
372 from the relative abundance of spores from obligate coprophilous fungi (*Sporormiella* +  
373 *Sordaria*); (g) summary diagram of temporal shifts in the composition of terrestrial vegetation,  
374 based on BOGS14 data.

375

#### 376 4.1.4 Cereals versus wild-type grasses

377 Over the entire 1300-year record, the fractional abundance of 60-85  $\mu\text{m}$  grass-pollen grains (as %  
378 of total Poaceae) is positively correlated with % total Poaceae pollen ( $r^2 = 0.157$ ,  $p < 0.01$ ,  $n = 90$ ;  
379 Fig. 4). No such correlation is found within zone BOGS-4 ( $r^2 = 0.002$ ,  $p = 0.87$ ,  $n = 25$ ), and the  
380 average fractional abundance of 60-85  $\mu\text{m}$  grass-pollen grains within that zone (0.36%) is well  
381 above that predicted by the full-record regression (0.27%). This indicates that although the 60-85  
382  $\mu\text{m}$  fraction may always contain a certain amount of wild-type grass pollen, its near-continuous  
383 presence in above-average amounts within zone BOGS-4 does indeed reflect the occurrence of  
384 indigenous cereal farming in the wider Lake Bogoria region.



385  
 386 **Fig. 4** Percentage (%) of 60-85  $\mu\text{m}$  Poaceae pollen grains versus the total % abundance of  
 387 Poaceae pollen, with symbol colors representing the successive pollen zones. Also shown are the  
 388 linear regression for all pollen zones (black line), and the average values ( $\pm$  SE) of each pollen  
 389 zone separately (colored crosses).

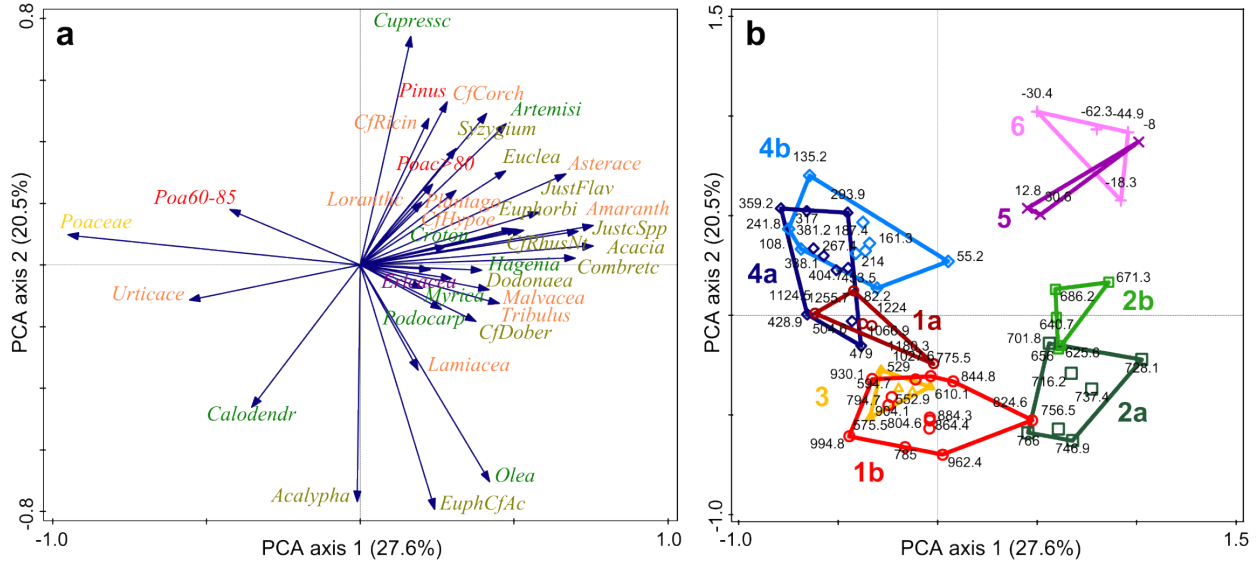
390

## 391 4.2 Multivariate analyses of vegetation and fire dynamics

### 392 4.2.1 Temporal dynamics in vegetation composition

393 PCA ordination biplots show the first two dimensions of the stratigraphic distribution of the 30  
 394 most diagnostic terrestrial pollen taxa in multivariate space (Fig. 5a), and changes in terrestrial  
 395 vegetation composition through time (Fig. 5b). Together these two dimensions represent almost  
 396 half (48.14%) of the observed variation in pollen assemblages. Dominant arboreal woodland taxa  
 397 (*Acacia*, Combretaceae, *Euclea*, *Euphorbia*, *Justicia* spp. incl. *J. flava*, cf. *Rhus natalensis*,  
 398 *Syzygium*), as well as several important herbs (Amaranthaceae, cf. *Corchorus*, cf. *Hypoestes*)  
 399 show close association with the *Acacia* wooded grassland. However, they are also associated with  
 400 the cultivated trees *Pinus* and Cupressaceae (partim) and herbs such as Asteraceae, cf. *Ricinus*

401 and *Plantago*, commonly interpreted as “disturbance” indicators (either natural or  
402 anthropogenic). The important Afromontane trees *Olea* and *Podocarpus* plot separately. Poaceae,  
403 cereals (Poaceae 60-85  $\mu\text{m}$ ), Urticaceae/Moraceae and cf. *Calodendrum* are also plotted in a  
404 separate group. With Poaceae being the dominant vector along PCA axis 1 (27.6% of the total  
405 variation), this first dimension of historical changes in pollen assemblages seems to reflect the  
406 gradient between open grassland (negative PCA 1 scores) and the more wooded biomes (positive  
407 PCA1 scores). The dominant vectors along PCA axis 2 (20.5% of total variation) are *Acalypha*  
408 and *Olea* on the negative side and Cupressaceae along with various “disturbance” indicators on  
409 the positive side, reflecting a gradient of increasing alteration of the vegetation. In the samples  
410 biplot (Fig. 4b), we note a shift along PCA axis 1 from the dry-phase open grassland vegetation  
411 of pollen zones BOGS-1a and BOGS-1b (mostly negative PCA1 scores) to the more wooded  
412 wetter-phase vegetation prevalent during BOGS-2a and BOGS-2b (positive PCA1 scores), and  
413 back to the dry-phase vegetation of BOGS-3, with all these assemblages having negative to  
414 neutral PCA2 scores. These shifts in PCA1 scores are mainly driven by abundance changes in  
415 Poaceae and in the savanna woodland taxa *Acacia*, *Justicia* spp., *J. flava*, Combretaceae and  
416 Amaranthaceae. Minor shifts along PCA2 mainly reflect variation in percent abundance of the  
417 Afromontane tree *Olea*. From BOGS-4 onward we see movement toward the positive side of  
418 PCA2, starting with the increase in Poaceae 60-85  $\mu\text{m}$  and declines in *Acalypha* and *Olea* (upper  
419 portion of BOGS-4a, and BOGS-4b) and followed by the increase in Cupressaceae and  
420 appearance of *Pinus* (BOGS-5 and BOGS-6). Simultaneously, the pollen assemblages also shift  
421 again from a dry-phase vegetation type (BOGS-4; negative PCA1 scores) to wetter-phase  
422 vegetation types (BOGS-5 and BOGS-6; positive PCA1 scores).



423  
 424 **Fig. 5** Principal Component Analysis (PCA) of the temporal distribution of pollen taxa in  
 425 sediment sequence BOGS14. (a) Species plot with color coding according to vegetation type, as  
 426 in Fig. 2. (b) Sample plot with samples labelled by age, and grouped using colored polygons to  
 427 demarcate the pollen zones, as in Fig. 3.

428

429 *4.2.2 Fire-vegetation interaction*

430 RDA analysis of the pollen-assemblage data with charcoal influx as single explanatory variable  
 431 indicates that fire (frequency and/or intensity) is responsible for only up to 10.5% of total  
 432 observed variance in past vegetation composition, which is modest but still significant ( $p < 0.01$ ).  
 433 The level of variance is in agreement with variance explained by fire elsewhere in Kenya and in  
 434 other fire-prone ecosystems (Colombaroli et al., 2009, 2018). Charcoal influx, interpreted here as  
 435 proxy for the magnitude of biomass burning, is positively associated with the percent pollen  
 436 abundances of the Afromontane forest tree cf. *Calodendrum* ( $r^2 = 0.25$ ,  $p < 0.001$ ) and woodland  
 437 tree *Acalypha* ( $r^2 = 0.25$ ,  $p < 0.001$ ), and negatively with Cupressaceae ( $r^2 = 0.27$ ,  $p < 0.001$ ) and  
 438 cf. *Ricinus* ( $r^2 = 0.28$ ,  $p < 0.001$ ). Considering the low explanatory power of charcoal in our  
 439 analysis these associations may however be fortuitous. Charcoal influx is also positively  
 440 associated with temporal variation in the percent Poaceae pollen, as could be expected, but this

441 correlation is modest at best ( $r^2 = 0.06$ ,  $p = 0.05$ ). Notably, charcoal influx has no relationship  
442 with the fraction of cereal-derived grass-pollen grains ( $r^2 = 0.00$ ,  $p = 0.93$ ).

#### 443 4.3 Landscape history as recorded in the northern basin of Lake Bogoria

444 The pollen record of the northern basin (BOGN14) covers only the last 440 years, but has a  
445 higher temporal resolution than BOGS14 because of the higher rate of sediment accumulation,  
446 particularly since the mid-20th century (De Cort et al., 2018). CONISS defines four pollen zones  
447 (Fig. 6), of which the boundary ages generally correspond well to those of the BOGS14 sequence  
448 (Fig. 2). The transition between BOGN-1 and BOGN-2 is placed around 1690 CE, almost coeval  
449 with the BOGS-4a/BOGS-4b transition dated to *ca* 1670 CE. The BOGN-2/BOGN-3 transition  
450 reflects the start of the savanna woodland expansion around 1850 CE evident at the top of  
451 BOGS-4b, shown through increases in *Acacia*, *Combretaceae*, *Justicia* spp. and *Amaranthaceae*.  
452 There is also a deep split in the CONISS cluster diagram around 1910 CE, i.e. coeval with the  
453 BOGS-4/BOGS-5 transition, justifying the division of BOGN-3 in two sub-zones. One of the  
454 prominent changes creating this sub-division is the abrupt rise in *Cupressaceae*, which also  
455 display a prominent increase across the BOGS-4/BOGS-5 transition. The most recent significant  
456 change in the north-basin pollen assemblage, the BOGN-3/BOGN-4 transition, is placed at *ca*  
457 2000 CE, several decades later than the BOGS-5/BOGS-6 transition, which is dated to *ca* 1965  
458 CE. Nevertheless, the main temporal trends in the pollen record of Lake Bogoria's northern basin  
459 are similar to our findings from the south-basin record 15 km away. Grasses (*Poaceae*) peak  
460 around 1800 CE at both sites, in BOGN14 with values up to 70%. *Sporormiella* displays its first  
461 notable increase *ca* 1630 CE (~50 years earlier than in BOGS14), followed by a strong increase  
462 ~200 years later from around 1850 CE, similar to BOGS14. Contrasting with BOGS14, also

463 *Sordaria* is recorded almost continuously since its first appearance in the late 17<sup>th</sup> century CE  
464 (Fig. 6).



466 **Fig. 6** Stratigraphic distribution of selected pollen taxa (all >1% of the terrestrial pollen sum) in  
467 the BOGN14 sediment sequence from the northern basin of Lake Bogoria, in relation to sediment  
468 age (De Cort et al., 2018) and pollen-based stratigraphic zonation (CONISS; Grimm, 1987).  
469 Taxon abundance is presented as percentage (%) based on the terrestrial pollen sum (black  
470 curves; 10x exaggeration in white), with taxa grouped per vegetation type. A summary diagram is  
471 shown on the left. Pollen from wetland taxa and fungal spores are expressed as percent of the  
472 terrestrial pollen sum but not included in it.

473

474 The pronounced maxima in *Sporormiella* and *Sordaria* (and also *Coniochaeta*) dated to *ca* 1900  
475 CE are recorded in a depth interval with low total pollen count (Fig. 6), thus these particular  
476 peaks are likely an artifact of poor pollen preservation at that level. Poaceae grains of 60-85  $\mu$ m  
477 are (almost) continuously present throughout the BOGN record (i.e., since at least *ca* 1575 CE),  
478 again consistent with BOGS, except that they persist into the 20<sup>th</sup>-century sediments (BOGN-3b)  
479 and become rare only after *ca* 2000 CE (BOGN-4). The cultivated taxa maize (i.e., Poaceae >85  
480  $\mu$ m) and *Pinus* both appear in this record from around 1950 CE; in the south-basin record *Pinus*  
481 appears in the late 1960s, whereas the only identified maize grain is dated to the 1990s. Finally,  
482 *Dodonaea* increases sharply in the last two decades (BOGN-4), a pattern highly similar to that in  
483 the south-basin record (top of BOGS-6). One notable difference between the recent portions of  
484 the two records concerns the Cupressaceae. In the south basin, the sharp and uniquely prominent  
485 increase in Cupressaceae from the 1960s onwards helps define the BOGS-5/BOGS-6 transition,  
486 whereas in the north basin Cupressaceae never exceed their pre-20<sup>th</sup> century abundances, and  
487 even experience a significant decrease since *ca* 2000 CE. Another notable difference is the  
488 presence of spores of the arbuscular mycorrhizal fungus *Glomus* in the north basin, first in a  
489 sediment layer deposited around 1850 CE and then more commonly in sediments deposited since  
490 the 1970s and until the present (Fig. 6). Living symbiotically in the root systems of terrestrial  
491 plants, the fossil spores of *Glomus* are indicative of soil erosion (van Geel et al., 1989). Its

492 occurrence at the top of the north-basin pollen record (top of BOGN-3b plus BOGN-4) is directly  
493 associated with the exponential increase in the rate of sediment accumulation in that basin (De  
494 Cort et al., 2018; Fig. 3c), reflecting rapidly accelerating soil erosion in the Sandai-Waseges  
495 River drainage since the 1970s. *Glomus* spores are lacking from BOGS14 (Fig. 2), because this  
496 plume of excess sediment enters Lake Bogoria from the north (Fig. 1a) and settles mostly within  
497 the north basin (Fig. 6). Because the areas drained by the ephemeral streams which enter the  
498 south basin are largely situated within the boundaries of Lake Bogoria National Reserve (Fig. 1a)  
499 they carry very little eroded soil. Excepting these topical differences, overall the north-basin  
500 pollen record of Lake Bogoria is equivalent to the last four centuries of its longer south-basin  
501 record, and can be considered to provide a close-up view of the latter.

## 502 **5. Discussion**

### 503 5.1 Vegetation response to climate variability

504 Modern-day potential natural vegetation in the wider Lake Bogoria region (Fig. 1b) consists of a  
505 mosaic of grass and shrub savanna, woodland, and open and closed canopy forest (Bontemps et  
506 al., 2011), i.e. it covers a wide portion of the East African grassland-to-forest ecotone. Our 1300-  
507 year pollen record documents past vegetation dynamics around Lake Bogoria covering the same  
508 range of vegetation types. Using percent Poaceae pollen as proxy for the degree of canopy  
509 openness in the grass-dominated ecosystems, the values between 40% and 75% found in this  
510 record are indicative of vegetation ranging from savanna woodland with relatively closed canopy  
511 to open grassland with isolated trees (Vincens et al., 2006; Ssemmanda et al., 2014). Many  
512 savanna trees and shrubs are insect-pollinated and therefore underrepresented in pollen records  
513 (Hamilton, 1972). However, the regionally important *Acacia*, *Dodonaea* and Combretaceae are

514 all sufficiently well-represented in the Lake Bogoria record to trace changes in their populations  
515 through time.

516 Previous reconstructions of past vegetation dynamics in the Lake Bogoria region documented a  
517 vegetation structure broadly similar to our findings. The only existing long pollen record from  
518 Lake Bogoria (Vincens, 1986) lacks sufficient temporal resolution to trace detailed landscape  
519 changes over the last few millennia, but shows comparable regional vegetation dominated by  
520 grasses (50-80%) with *Podocarpus*, *Juniperus* and *Olea* as dominant Afromontane trees; and  
521 typical Somalia-Masai savanna vegetation with *Acacia*, *Dodonaea* and a strong presence of  
522 *Justicia*. Pollen records from nearby locations such as Loboï Swamp (Ashley et al., 2004; Driese  
523 et al., 2004), Lake Baringo (Kiage & Liu, 2009) and Lake Solai (Goman et al., 2017) cover only  
524 part of the last millennium and/or suffer from stratigraphic hiatuses. Due to the depositional  
525 nature of these sites, the vegetation reconstructions also mainly reflect local to extra-local  
526 ecosystem dynamics and do not shed much light on climate-human-landscape interaction in the  
527 wider region. A reconstruction of vegetation history on the Laikipia plateau to the east of Lake  
528 Bogoria shows that it was covered by *Podocarpus* forest and *Acacia* bushland until about 2000  
529 years ago, which was gradually replaced by fire-adapted grassland with *Justicia* so that only  
530 fragments of the earlier vegetation remain today (Taylor et al., 2005).

531 Our 1300-year pollen record reveals two major periods of regional forest and woodland  
532 expansion, first from *ca* 1100 to 1330 CE and more recently from *ca* 1870 CE until the present.  
533 Both periods see net increases of woody taxa within the local *Acacia* wooded grassland and in  
534 more distant areas of Afromontane forest. There is also a large concurrent increase in herbaceous  
535 taxa, at the expense of Poaceae. The older period comprises three distinct episodes of  
536 woodland/forest expansion, one near the top of pollen zone BOGS-1b and two forming the bulk

537 of BOGS-2. All three episodes, respectively peaking around 1125, 1220 and 1280 CE,  
538 correspond with phases of high lake level (De Cort et al., 2018; Fig. 3a), strongly suggesting a  
539 primary vegetation response to temporary increase of the region's climatic moisture balance.  
540 Notably, the only tree that consistently increases during all three moist-climate episodes is  
541 *Acacia*. Otherwise, a different combination of woody taxa respond to increased moisture during  
542 each individual episode. During the first, the greatest increases are in *Podocarpus*, Combretaceae  
543 and *Dodonaea* followed by *Acalypha*; during the second, increases of *Olea*, *Justicia* and  
544 *Dodonaea* are followed by Combretaceae; and during the third, a further rise in *Justicia* is  
545 accompanied first by *Euphorbia* and then by *Olea* (Fig. 2). Previously, a brief episode of  
546 forest/woodland expansion had also occurred in the late 10th century CE, with increases in  
547 *Podocarpus*, *Acalypha* and *Euphorbia* cf. *acalyphoides* (Fig. 2) also at that time coinciding with  
548 a (modest) positive lake-level shift (Fig. 3a). The expansions of *Acacia* and *Euphorbia* cf.  
549 *acalyphoides* suggest a thickening of woody vegetation in savanna proper, whereas those of  
550 *Acalypha* and *Podocarpus* may reflect a temporary shift in the forest/woodland ecotone. A  
551 positive response of herbaceous taxa to moister climatic conditions seems to have occurred only  
552 during the two lake high-stands between *ca* 1175 and 1330 CE, and involved the Amaranthaceae  
553 as well as Asteraceae and Lamiaceae, many of which constitute savanna woodland understory  
554 (Vincens et al., 2006); this strong display of herbaceous taxa helps delineate pollen zone BOGS-  
555 2. The notably modest responsiveness of *Podocarpus* to both climatic (and anthropogenic)  
556 pressures over the 1300-year record (mean abundance  $11 \pm 2\%$  throughout BOGS14) may  
557 indicate that its pollen has always predominantly been delivered to Lake Bogoria by long-  
558 distance transport, from areas of adjacent highlands (perhaps as far as the Aberdare Range, 80-  
559 100 km to the southeast) that are topographically sufficiently diverse to generate compensating  
560 positive and negative responses of the dry-forest biome to regional moisture-balance changes.

561 The younger period of forest/woodland expansion (*ca* 1870 until today), represented by the top of  
562 pollen zone BOGS-4b plus BOGS-5 and BOGS-6 (Fig. 2), similarly correlates with generally  
563 high lake levels of Lake Bogoria since the start of the 19<sup>th</sup> century (De Cort et al., 2018; Fig. 3a).  
564 Among forest trees, the responses of *Podocarpus* and *Olea* are relatively weak; instead the  
565 strongest increases from early in this period are in Cupressaceae (still on account of native  
566 *Juniperus procera*) and the relatively uncommon *Artemisia* and *Hagenia* (Fig. 2). Otherwise the  
567 initial vegetation changes follow the same general pattern as in the previous wet period, with  
568 strongest increases in taxa associated with *Acacia* wooded grassland: *Acacia* itself, *Justicia* spp.  
569 and Amaranthaceae. Toward the top of BOGS-5 the pollen record seems to reveal a temporary  
570 decline in forest and woodland components dating to the early 20<sup>th</sup> century. Coeval with a  
571 prolonged regression of Lake Bogoria (Fig. 3a) and other lake-level declines throughout Kenya  
572 (Verschuren, 2004), this episode of climatic drying coincided with a period of colonial land  
573 expropriation in the former ‘White Highlands’ of central Kenya (Verschuren et al., 1999).  
574 However, apparent reduction in the forest/woodland component at that time may also, at least in  
575 part, be a statistical effect resulting from strong increases in the disturbance indicators  
576 Amaranthaceae and Asteraceae (Fig. 2). In any event, starting *ca* 1965 CE (pollen zone BOGS-6)  
577 a last forest/woodland expansion is recorded, this one almost entirely due to increases in  
578 Cupressaceae (most certainly the introduced timber cypress) and the encroaching native shrub  
579 *Dodonaea*. With planted *Pinus* also appearing in the record, Poaceae are reduced to all-time low  
580 values of respectively 20% and 23% in the modern-day pollen assemblages of Lake Bogoria’s  
581 southern and northern basins.

582 Corroborating the above interpretation of vegetation history, the results of PCA analysis show  
583 that the greatest portion of explained variation in pollen-assemblage composition over the past

584 1300 years (PCA1 = 27.6%) is related to shifts between open grassland and more closed-canopy  
585 dry vegetation, driven mainly by abundance changes in Poaceae and the savanna woodland taxa  
586 *Acacia*, *Justicia*, Combretaceae and Amaranthaceae in response to climate-driven changes in  
587 available moisture (Fig. 3a). Importantly, the PCA results show that after the first documented  
588 period of forest/woodland expansion between *ca* 1100 and 1330 CE, regional vegetation returned  
589 to its pre-existing composition associated with somewhat drier climate conditions.

590 Closed-canopy dry Afromontane forest can be found today on the Laikipia Plateau (Taylor et al.,  
591 2005), in Lembus Forest on the western escarpment, and in small patches within the Bogoria  
592 catchment (Vincens et al., 1986; Fig. 1c). Excluding Cupressaceae, the Afromontane component  
593 represents 9% and 12%, respectively, of the modern-day pollen assemblage in the northern and  
594 southern basins, and in the latter it has varied between 14% and 54% during the past 1300 years  
595 of recorded history. This is because its prominent tree taxa *Podocarpus* and *Olea* tend to be over-  
596 represented in pollen assemblages, as their pollen is delivered to lakes and swamps by long-  
597 distance aerial transport (Taylor et al., 1999). Thus, the percent abundance of the Afromontane  
598 component should not be taken to reflect the percent areal cover of closed-canopy forest on the  
599 regional landscape (Prentice & Webb, 1986; Ssemmanda et al., 2014). Nevertheless, as long as  
600 the magnitude of this over-representation can be considered constant through time, temporal  
601 changes in percent abundance of the Afromontane component can be considered to reflect true  
602 shifts of the forest-woodland ecotone across the regional landscape. One important caveat is that  
603 pollen can also be transported over large distances by rivers, so that temporal changes in the  
604 hydrography of lake catchments can create signatures of apparent vegetation change without any  
605 real change in areal coverage (Prentice, 1985). Specifically, in our record the correlation between  
606 forest/woodland expansion and high lake-level stands might be due partly to enhanced influx of

607 forest and woodland pollen from highland areas within the Lake Bogoria catchment during  
608 episodes of greater streamflow. We consider the impact of this long-distance transport as  
609 relatively minor, for three reasons. First, past vegetation changes reconstructed from BOGN14  
610 for the most part echo the results from BOGS14, highlighting the robustness of common  
611 temporal trends in the region's vegetation revealed by both records, notwithstanding the distance  
612 of 15 km between these sites. Second, since inflow via the Sandai-Waseges River enters Lake  
613 Bogoria from the north (Fig. 1a) and reaches the southern basin only during high-stands (De Cort  
614 et al., 2018), the ratio between forest/woodland and Poaceae pollen, if it has a strong riverine-  
615 influx signature, should on average be higher in BOGN14 than in BOGS14, which is not the case  
616 (80% versus 100% ( $p = 0.4$ ) over the past 440 years). Finally, vegetation response to the inferred  
617 shift toward a wetter climate between *ca* 1100 and 1330 CE displays distinct differences during  
618 each separate episode of forest/woodland expansion, with different forest and woodland taxa  
619 enjoying the most prominent increases. Had the increases in forest/woodland been due mostly to  
620 higher influx rather than vegetation change, we would expect the patterns to be more similar to  
621 each other. Thus, the combined evidence suggests that although the influence of changing river  
622 influx cannot be dismissed, the largest portion of documented increases in woodland and forest  
623 pollen reflects shifts in vegetation ecotones both within and beyond the Lake Bogoria catchment.

## 624 5.2 History of human influence on Kenya Rift Valley ecosystems

625 The history and archaeology of human occupation in central Kenya has been studied in some  
626 detail. Pastoralist communities are thought to have been present in East Africa from *ca* 4800 BP,  
627 extending from Lake Turkana into the Rift Valley (Hildebrand et al., 2018), but the  
628 archaeological record of this southward expansion remains scarce until *ca* 3000 years ago (Lane,  
629 2013; Petek, 2018). Agriculture is thought to have spread from the Lake Victoria region into the

630 central Rift Valley by the mid-first millennium CE, first evidenced by botanical remains found *ca*  
631 30 km west of Lake Nakuru (Ambrose et al., 1984). The area around Lake Baringo, probably  
632 including Lake Bogoria, was at that time occupied by producers of Turkwel ceramics, who were  
633 principally herders who also hunted and fished. From around the time that human influence can  
634 first be discerned in the Bogoria pollen record (cf. below), archaeological sites south of Lake  
635 Baringo indicate that well-watered locations surrounding lakes Baringo and Bogoria were most  
636 likely inhabited by farming and/or hunting-gathering groups. Pastoral communities mostly  
637 occupied drier Rift Valley areas to the south and west, utilizing pasture and swamps near the  
638 lakes only seasonally (Petek, 2018). Pastoralism was also well established eastward of the lakes,  
639 on the Laikipia Plateau (Lane, 2013). As indicated by our 1300-year paleo-environmental  
640 reconstruction, the magnitude and diversity of influences on the region's natural resources  
641 exerted by the various people inhabiting the Bogoria drainage basin has steadily increased  
642 through time, in six more or less distinct phases.

#### 643 *5.2.1 First phase: limited human influence pre-1430 CE*

644 In the PCA biplot showing the compound trends in pollen-assemblage composition through time  
645 (Fig. 3b), shifts along PCA axis 1 reflects vegetation response to changes in climatic moisture  
646 balance while shifts along PCA axis 2 reflects the relative intensity of human influence. In the  
647 first *ca* 700 years of the Lake Bogoria record, vegetation changes from a dry-phase open  
648 grassland (zone BOGS-1) to more wooded wet-phase vegetation (BOGS-2) and back to dry-  
649 phase open grassland (BOGS-3), with all these pollen assemblages having negative to neutral  
650 PCA2 scores, and thus little evidence of anthropogenic disturbance. Also in the other proxies, the  
651 pre-1430 CE portion of the record shows little evidence of human landscape modification.  
652 Charcoal influx has a mostly inverse relationship with hydroclimatic variation in zones BOGS-1

653 through BOGS-3 (Figs. 3d and 3a), indicating that savanna fires were predominantly under  
654 climatic control; and that biomass burning was promoted by relative drought, as is expected to  
655 occur in areas near the forest/grassland boundary (Colombaroli et al., 2014). The first modest  
656 presence of *Sporormiella* between *ca* 1175 and 1330 CE postdates archaeological sites associated  
657 with Turkwel herders (*ca* 200-1100 CE; Petek, 2018), while no recorded sites date specifically to  
658 the period 1175-1330 CE. In the absence of other proxy indicators of human activity in this part  
659 of the record, the most conservative explanation for the early appearance of *Sporormiella* is a  
660 greater proliferation of fungi on wildlife rather than domesticated herbivore dung during the  
661 relatively moist climate conditions which then prevailed (Fig. 3a).

#### 662 *5.2.2 Second phase: expanding agricultural activity and landscape clearing*

663 The first suspected ecological indication of humans being present in the landscape surrounding  
664 Lake Bogoria is the general shift in pollen-assemblage composition along PCA axis 2 (Fig. 5b),  
665 starting modestly in zone BOGS-4 (of which the base is dated to *ca* 1430 CE) and becoming  
666 stronger in BOGS-5 (from *ca* 1910 CE) and BOGS-6 (from *ca* 1965 CE). The first unambiguous  
667 proxy evidence of agricultural activity is the continuous presence, from *ca* 1500 CE, of Poaceae  
668 pollen in the size range 60-85  $\mu\text{m}$ , which we argue is disproportionately derived from indigenous  
669 cereals such as finger millet and sorghum and therefore indicative of farming being practiced in  
670 the Lake Bogoria region (cf. Results, section 4.1.4). Note that because of the positive correlation  
671 between the fraction of 60-85  $\mu\text{m}$  Poaceae grains and total Poaceae pollen (Fig. 4), elevated  
672 amounts of 60-85  $\mu\text{m}$  grass pollen are not *by themselves* an unambiguous indicator for cereal  
673 farming. Conversely, we cannot claim that the 60-85  $\mu\text{m}$  ‘cereal-type’ grains occurring earlier in  
674 the record, specifically during the relatively dry climatic periods represented by zones BOGS-1b  
675 and BOGS-3 (Figs. 2 and 4), are anything other than very large wild-type grass pollen.

676 Strikingly, between *ca* 1500 and 1870 CE, broadly the period when 60-85  $\mu\text{m}$  Poaceae pollen is  
677 more abundant than expected from wild-type distribution, the combined fraction of arboreal  
678 woodland pollen is only 4-8% (mean value 5%) whereas it is mostly >15% (7-25%) in the rest of  
679 the record, during both wet and dry climate phases (Fig. 2). This pattern is mostly due to a near-  
680 total loss of *Acalypha* after 1430 CE. Also during this same period the forest tree *Olea* is reduced  
681 to <10%, while it exceeds 15% in much of the rest of the record, again during both wet and dry  
682 climate phases. These patterns suggest that indigenous land-use practices in the Lake Bogoria  
683 region between the 15<sup>th</sup> and 19<sup>th</sup> centuries CE led to a general reduction of land covered by  
684 grassland-to-forest ecotonal vegetation – where *Acalypha fruticosa* can be found – due to  
685 clearance of mid-elevation areas with fairly densely wooded savanna and the fringe of closed-  
686 canopy dry forest. *A. fruticosa* having many useful applications, it may have been removed  
687 selectively. Considering the responsiveness of *Olea* to climate-driven moisture-balance changes  
688 in the early part of the record, this tree may have been particularly common in the patches of  
689 forest within the Bogoria catchment that were cleared for farming or wood collection.

### 690 5.2.3 Third phase: increased animal husbandry, and modification of the fire regime

691 Our dung-fungus evidence indicates that animal husbandry, as a livelihood strategy with  
692 significant ecological impact in the Lake Bogoria region, is attested from the mid-17<sup>th</sup> century  
693 onwards. In temporally dynamic ecosystems, such as our semi-arid tropical study area, natural  
694 processes can exert substantial control on dung-fungus growth and distribution (Gelorini et al.,  
695 2012; Baker et al., 2013). Specifically, past episodes of wetter/drier climate likely  
696 increased/decreased the prevalence of damp micro-habitat conditions which tend to  
697 promote/restrict the growth of fungi. Consequently we surmise that the contrast between  
698 moderately high abundances of obligate coprophilous fungi in pollen zone BOGS-2, versus very

699 low abundances in pollen zones BOGS-1, BOGS-3 and the base of BOGS-4, is within the  
700 expected variability resulting from entirely natural variation in local habitat suitability for the  
701 fungi themselves, rather than from changes in herbivore populations. Only spore abundances  
702 clearly exceeding this natural variability can be considered as created by livestock present along  
703 the shores of Lake Bogoria. From *ca* 1630-1670 CE onwards, the abundances of *Sporormiella*  
704 (and of *Sordaria*, in the north basin) increase above their previous mean dry-phase abundance (cf.  
705 pollen zone BOGS-2; Fig. 2), and are therefore interpreted as being linked to domestic cattle.  
706 Further, as this mid-17<sup>th</sup> century *Sporormiella* rise coincides with the certified presence of cereal  
707 grains, it most likely reflects mixed farming and animal husbandry, the latter partly by  
708 pastoralists utilizing the lake area on a seasonal basis (Lane, 2013; Petek, 2018).

709 The broadly inverse relationship between charcoal and moisture balance culminates in a broad  
710 charcoal maximum dated to *ca* 1550-1600 CE (Fig. 3d). This is consistent with the prevailing dry  
711 climate conditions (Fig. 3a) but may also be attributed to, or enhanced by, the clearance of natural  
712 vegetation due to the then expanding farming practices. Notably, the inverse correlation between  
713 fire and moisture balance continues for another ~200 years until *ca* 1800 CE, but with overall  
714 lower amounts of biomass burning both during wetter and drier climatic episodes (Fig. 3d).  
715 Coeval with the now firm proxy evidence for farming activity, we surmise that this reduction in  
716 overall biomass burning reflects the suppression of fire which occurs when land conversion for  
717 agriculture becomes significant at the landscape scale (Colombaroli et al., 2014). Any human-  
718 assisted burning that did occur was most likely associated with additional plot clearance for  
719 farming, not burning by pastoralists to improve fodder (e.g., Bird & Cali, 1998). In fact, the  
720 contemporaneous groups of specialized pastoralists probably dwelled mostly in Rift Valley areas  
721 too dry to make deliberate burning useful.

#### 722 5.2.4 Fourth phase: establishment of irrigation agriculture

723 Historical information and archaeological evidence indicate that from the 1830s CE onwards,  
724 Ilchamus groups occupying the land between lakes Baringo and Bogoria established a large-scale  
725 irrigation agriculture system with the intention of surplus food production, while more traditional  
726 rain-fed agriculture was restricted to wetter zones on the Rift Valley flanks (Anderson, 2016;  
727 Petek & Lane, 2017; Petek, 2018). In the Lake Bogoria record, this development appears to be  
728 reflected in the much greater abundance of cereal pollen being recovered from north-basin  
729 sediments dated to the second half of the 19<sup>th</sup> century, compared to south-basin sediments (Fig.  
730 3); and the first appearance of certified maize pollen *ca* 1880 CE. The charcoal record is also  
731 broadly consistent with increased agricultural activity. The prominent but short-lived charcoal  
732 peak dated to *ca* 1820 CE coincides, within dating precision, to the end of a severe early 19<sup>th</sup>  
733 century drought that affected much of East Africa (Verschuren et al., 2000; Bessems et al., 2008;  
734 Nash et al., 2016). Attracting Maa and Kalenjin pastoralists to the area immediately north of Lake  
735 Bogoria, the resulting increase in demographic pressure caused social upheaval and  
736 reconfiguration (Anderson, 2016). We therefore surmise that the 1820 CE charcoal peak is most  
737 likely anthropogenic, and reflects land clearance by Il Chamus farmers in low-lying valley areas  
738 for the purpose of irrigation agriculture (Anderson & Bollig, 2016). The characteristic pattern of  
739 an initial peak of biomass burning followed by strong reduction of fire has also been commonly  
740 reported from episodes of vegetation clearance in extra-tropical regions, at local (e.g., Bradshaw  
741 & Lindblath, 2005; Colombaroli et al., 2013) to near-global scales (Marlon et al., 2008). This  
742 particular charcoal peak is accompanied by a prominent shift to more fine-grained clastic  
743 sedimentation, the first indication of soil loss in clay-rich areas of the Sandai River catchment  
744 (De Cort et al., 2018; Fig. 3b). In the north basin this shift is abrupt, as expected given its direct

745 hydrographic connection with the source area of this clay. In the south basin the shift starts  
746 around 1820 CE but ramps up gradually to peak around 1900 CE (Fig. 6), likely because the lake  
747 level was initially too low for effective inter-basin redistribution of suspended clays. Importantly,  
748 excluding this brief peak around 1820 CE, 19<sup>th</sup>-century biomass burning never reached the levels  
749 commonly attained during the earlier part of the Bogoria record.

750 Not only crop agriculture but also animal husbandry expanded through much of the 19<sup>th</sup> century  
751 CE. The prominent rise in *Sporormiella* from *ca* 1850-1870 CE onwards, to abundances well  
752 above their previous mean wet-phase abundance (Fig. 6), is consistent with historical evidence  
753 for strong expansion of cattle pastoralism between the 1830s and 1870s (Anderson & Bollig,  
754 2016). However, at least in its initial phase the dung-fungus rise may have been produced partly  
755 by wild herbivores, since large herds of buffalo, wildebeest and other large ungulates are  
756 historically well attested for the late 19<sup>th</sup> century while the cattle population tended to fluctuate  
757 due to diseases such as rinderpest (Little, 1996). This period was also marred by inter-community  
758 conflict; in particular the Loikop wars between different Maasai sections competing for the best  
759 grazing land (Anderson, 2016).

#### 760 *5.2.5 Fifth phase: return of wetter climate and reduction of crop agriculture*

761 With the return of wetter climate conditions in the mid-19<sup>th</sup> century, there was renewed  
762 expansion of forest/woodland ecotone vegetation, signifying an overall reduction of crop  
763 agriculture on the Rift Valley flanks (i.e., higher-elevation portions of the Bogoria catchment).  
764 *Acalypha*, which had become scarce coincident with the appearance of cereal pollen four  
765 centuries before, failed to recover (Fig. 2). However, this was compensated by notable increases  
766 in Combretaceae, *Justicia* spp. and cf. *Dobera/Nuxia* from the mid-19<sup>th</sup> century onwards (Fig. 2).

767 As regards the former two taxa, the resulting higher percent abundances are largely sustained  
768 until the present (top of BOGS-4, plus BOGS-5 and BOGS-6), notwithstanding the three- to  
769 fourfold expansion of Cupressaceae (cypress plantations) and invasive *Dodonaea* in recent  
770 decades (Fig. 2). Complete lack of 60-85  $\mu\text{m}$  Poaceae grains from *ca* 1910 CE onward in the  
771 south-basin record probably also reflects this reduction farming compared with earlier times,  
772 except that also the amount of total Poaceae pollen counted in this section of the sequence is too  
773 low to state this with certainty. In notable contrast, 60-85  $\mu\text{m}$  grass pollen is persistently present  
774 throughout 19<sup>th</sup> and 20<sup>th</sup> century sediments deposited in the north basin (Figs. 3 and 6), testifying  
775 to a general shift of cereal farming to the irrigated cropland in low-lying portions of the Bogoria  
776 catchment. By the start of British colonial rule around the turn of the 20<sup>th</sup> century, cattle  
777 pastoralism had become the dominant production system in the wider Baringo-Bogoria region,  
778 including areas to the south of Lake Bogoria (around Lake Solai; Fig. 1a) occupied in the 1910s  
779 and 1920s by specialized pastoralists migrating from the Tugen Hills area west of Lake Baringo  
780 (Little, 1992; Anderson, 2002; Petek, 2018),

#### 781 *5.2.6 Sixth phase: intensive land use leading to widespread soil erosion*

782 Following over half a century of rapid growth in cattle herding (i.e. the period of persistently high  
783 *Sporormiella* abundances in zone BOGS-5; Figs. 2 and 3), livestock numbers eventually  
784 exceeded the carrying capacity of the land, resulting in widespread vegetation degradation  
785 (Johansson & Svensson, 2002). Most pertinently, since the 1950s open grassland in the Baringo  
786 rangelands was increasingly replaced by *Acacia* bushland, exacerbated by a burning prohibition  
787 (Vehrs, 2016; Vehrs & Heller, 2017). This expansion of *Acacia* bushland is likely responsible for  
788 the strong reduction in Poaceae pollen and rises in *Acacia*, *Justicia flava* and Asteraceae from the  
789 1930s onwards (Fig. 2). Moreover, apparent reduction of the latter three taxa in the pollen

790 assemblages after *ca* 1965 CE may well be an artefact of the strong expansions of exotic *Pinus*  
791 and Cupressaceae, and of native disturbance taxa such as *Plantago*, *Ricinus* and *Dodoniaea* (Fig.  
792 2). In recent decades many low-lying areas around Lake Baringo and Loboï Swamp (immediately  
793 to the north of Lake Bogoria; Fig. 1b) have also suffered from encroachment by the exotic shrub  
794 *Prosopis juliflora* (mesquite; Mwangi & Swallow, 2008), an insect-pollinated plant related to  
795 *Acacia* but largely invisible in the pollen record.

796 Bond & Midgley (2000) implicated the anthropogenic rise in atmospheric CO<sub>2</sub> since the early  
797 19<sup>th</sup> century CE, and accelerating since the 1950s, in the historical trend toward greater tree cover  
798 observed in many tropical savannas. This trend specifically applies to mesic wooded savannas of  
799 the forest/grassland ecotone where fire is drought-controlled (Bond & Midgley, 2012), as is the  
800 case in our study area (sections 4.1.2 and 5.2.1). The question then arises whether rising CO<sub>2</sub> may  
801 have contributed to the historical expansion of tree cover across the Rift-Valley landscape as  
802 inferred from our Bogoria record. Combretaceae, *Justicia* spp. and cf. *Dobera/Nuxia* expanded  
803 from the mid-19<sup>th</sup> century onwards, followed by *Acacia* bushland from the mid-20<sup>th</sup> century.  
804 However, given the magnitude of alternative ecological drivers, i.e. an improving moisture  
805 balance from the 1830s onwards and 20<sup>th</sup>-century rangeland degradation due to overgrazing, we  
806 refrain from attributing any recorded changes in pollen-assemblage composition uniquely to the  
807 rise in atmospheric CO<sub>2</sub>.

808 Scarcity of open grassland prompted the region's pastoralists to switch from cattle to browsers  
809 such as goats and camels (Vehrs, 2016). Browsing by goats, in particular, further increased the  
810 pressure on this fragile valley-floor landscape by over-eating the vegetation and trampling its root  
811 systems. The logical consequence, then, was severe soil erosion and gully formation throughout  
812 the riparian lands surrounding Lake Baringo, including the lower Sandai River drainage towards

813 Lake Bogoria (Johansson & Svensson, 2002). Meanwhile in higher-elevation portions of the  
814 Sandai-Waseges drainage, where mixed subsistence farmers used to concentrate, rapid  
815 demographic growth and increased development of timber plantations reduced the acreage  
816 available for individual small-holdings (Anderson, 2002), so that land use intensified, few plots  
817 lay fallow at any one time, and also those soils became increasingly destabilized.  
818 Sedimentological analyses by De Cort et al. (2018) suggest that soil erosion in the upper Bogoria  
819 catchment, entirely outside Lake Bogoria National Reserve, is the principal cause for the order-  
820 of-magnitude increase in terrestrial sediment supply to Lake Bogoria since the 1970s (Fig. 3c).  
821 Soil eroded from such agricultural land is likely to contain elevated concentrations of  
822 coprophilous fungal spores derived from locally applied domestic herbivore dung. We surmise  
823 that the most recent peak in *Sporormiella* spores recorded in Lake Bogoria's north basin (but not  
824 south basin; Fig. 3c) may reflect this process rather than changes in large herbivore density  
825 nearby the lake, which grew slowly or stagnated at that time (Little, 1992; Anderson, 2002). This  
826 inference is supported by the coincidence of this *Sporormiella* peak with maximum abundance of  
827 *Glomus* spores, a root symbiont indicative of soil erosion (van Geel et al., 1989).

828 Considering the evident causal relationship between accelerated sedimentation in the north basin  
829 and land-use intensification over the past *ca* 50 years, it is tempting to link the elevated rate of  
830 sedimentation which occurred between *ca* 1600 and 1800 CE (Fig. 3c) with the multi-proxy  
831 evidence for indigenous farming during this period (Fig. 3d-f). However, as the texture of  
832 sediments deposited at the offshore core site remains unchanged throughout this period (Fig. 3b),  
833 we interpret these data as reflecting the focusing and re-deposition of sub-lacustrine mud during  
834 the contemporaneous low-stand episode (Fig. 3a; Verschuren, 1999). This low-stand impacted  
835 water depth (and hence sedimentation dynamics) in the north basin more strongly than in the

836 south basin because of its shallower lake bottom, while also restricting any new sediment load  
837 from the Sandai-Waseges entirely to the north basin (De Cort et al., 2018).

## 838 **6. Conclusion**

839 The regionally unique situation of depositional continuity, undisturbed accumulation and well-  
840 constrained chronology of the Lake Bogoria sediment record (De Cort et al., 2018) has permitted  
841 a detailed reconstruction of the history of human influences on the landscape of Kenya's central  
842 Rift Valley against the backdrop of natural, climate-driven ecosystem dynamics over the past  
843 1300 years. Our multi-proxy reconstruction reveals a succession of five phases of distinct human  
844 activity since *ca* 1430 CE, following a period of (at least) *ca* 700 years when the region's  
845 landscape consisted of a savanna-forest ecotone responding primarily to climate-driven shifts in  
846 moisture balance. The first unambiguous ecological signature of human activity occurs long after  
847 human presence is first attested archaeologically; and landscape evolution during the last six  
848 centuries reflected the continually shifting interplay between human activity, climate, and locally  
849 available land and water resources. Our results show that ecological impacts by indigenous  
850 human activity in this tropical African landscape became significant already *ca* 500 years before  
851 the start of the colonial period; however in contrast to many Mediterranean, temperate and boreal  
852 ecosystems (Lewis & Maslin, 2015), they supplanted natural processes as the dominant driver of  
853 vegetation dynamics only in the course of the 20<sup>th</sup> century, through the introduction of exotic  
854 trees and crops, fire suppression, scrub encroachment, and eventually widespread soil erosion  
855 since the 1960s resulting from intensified agriculture and overgrazing.

## 856 **Acknowledgements**

857 This research was conducted as part of the Marie Curie Initial Training Network ‘Resilience in  
858 East African Landscapes’ supported by the European Commission's 7th Framework Programme  
859 (Grant no. 606879) awarded to PL and DV. The sediment cores were made available through the  
860 Belgian Science Policy (Belspo) Brain-be project ‘Patterns and Mechanisms of Climate Extremes  
861 in East Africa’ (BR/121/A2/PAMEXEA), with additional fieldwork support by the Research  
862 Foundation Flanders (FWO). The fieldwork was executed with permits from the National  
863 Commission for Science, Technology and Innovation of Kenya (RRI/12/1/BS011/44) and the  
864 National Environmental Monitoring Authority (AGR/7/2010/0029), and the research materials  
865 were exported under Material Transfer Agreement A11/TT/1040 between the Kenya Wildlife  
866 Service, the University of Nairobi and Ghent University.

867 **Competing interest statement:** The authors declare to have no competing interests.

## 868 **References**

869 Ambrose, S.H., Collett, D.P., Marshall, F.B., 1984. Excavations at Deloraine, Rongai, 1978.

870 *Azania* 19, 79–104.

871 Andersen, S.T., 1979. Identification of wild grass and cereal pollen. *Danmarks Geologiske*

872 *Undersøgelse Årbog* (1978), 69–92.

873 Anderson, D., 2002. *Eroding the commons: the politics of ecology in Baringo, Kenya, 1890s–*

874 *1963*. James Currey Publishers, Oxford.

875 Anderson, D.M., 2016. The beginning of time? Evidence for catastrophic drought in Baringo in

876 the early nineteenth century. *J. East. Afr. Stud.* 10, 45–66.

877 Anderson, D.M., Bollig, M., 2016. Resilience and collapse: histories, ecologies, conflicts and

878 identities in the Baringo-Bogoria basin, Kenya. *J. East. Afr. Stud.* 10, 1–20.

879 Ashley, G.M., Maitima Mworira, J., Muasya, A.M., Owen, R.B., Driese, S.G., Hover, V.C.,  
880 Renaut, R.W., Goman, M.F., Mathai, S., Blatt, S.H., 2004. Sedimentation and recent  
881 history of a freshwater wetland in a semi-arid environment: Loboï Swamp, Kenya, East  
882 Africa. *Sedimentology* 51, 1301–1321.

883 Baker, A.G., Bhagwat, S.A., Willis, K.J., 2013. Do dung fungal spores make a good proxy for  
884 past distribution of large herbivores? *Quat. Sci. Rev.* 62, 21–31.

885 Becker, M., Alvarez, M., Heller, G., Leparmarai, P., Maina, D., Malombe, I., Bollig, M., Vehrs,  
886 H., 2016. Land-use changes and the invasion dynamics of shrubs in Baringo. *J. East. Afr.*  
887 *Stud.* 10, 111–129.

888 Bessems, I., Verschuren, D., Russell, J.M., Hus, J., Mees, F., Cumming, B.F., 2008.  
889 Palaeolimnological evidence for widespread late 18th century drought across equatorial  
890 East Africa. *Palaeogeogr. Palaeoclimatol. Palaeoecol.* 259, 107–120.

891 Bird, M.I., Cali, J.A., 1998. A million-year record of fire in sub-Saharan Africa. *Nature* 394, 767.

892 Blaauw, M., Christen, J.A., 2011. Flexible paleoclimate age-depth models using an  
893 autoregressive gamma process. *Bayesian anal.* 6, 457–474.

894 Blaauw, M., van Geel, B., Kristen, I., Plessen, B., Lyaruu, A., Engstrom, D.R., van der Plicht, J.,  
895 Verschuren, D., 2011. High-resolution 14C dating of a 25,000-year lake-sediment record  
896 from equatorial East Africa. *Quat. Sci. Rev.* 30, 3043–3059.

897 Bond, W.J., Midgley, G.F., 2000. A proposed CO<sub>2</sub>-controlled mechanism of woody plant  
898 invasion in grasslands and savannas. *Glob. Change Biol.* 6, 865–869.

899 Bond, W.J., Midgley, G.F., 2012. Carbon dioxide and the uneasy interactions of trees and  
900 savannah grasses. *Philos. T. Roy. Soc. B.* 367, 601–612.

901 Bonnefille, R., 1972. Associations polliniques actuelles et quaternaires en Ethiopie. Unpublished  
902 thesis, Université de Paris VI.

903 Bonnefille, R., Riollet, G., 1980. Pollens de savanes d'Afrique orientale. Editions du Centre  
904 National de la Recherche Scientifique, Paris.

905 Bontemps, S., Defourny, P., Bogaert, E.V., Arino, O., Kalogirou, V., Perez, J.R., 2011.  
906 GLOBCOVER 2009-Products description and validation report.

907 Bradshaw, R.H.W., Lindblath, M., 2005. Regional spread and stand-scale establishment of *Fagus*  
908 *sylvatica* and *Picea abies* in Scandinavia. *Ecology* 86, 1679–1686.

909 Burgess, T., Wingfield, M.J., 2001. Exotic pine forestry in the Southern Hemisphere: a brief  
910 history of establishment and quarantine practices. *S Afr. Forest. J.* 192, 79–83.

911 Caseldine, C.J., Turney, C., 2010. The bigger picture: towards integrating palaeoclimate and  
912 environmental data with a history of societal change. *J. Quat. Sci.* 25, 88–93.

913 Chaturvedi, M., Yunus, D., Datta, K., 1994. Pollen morphology of *Sorghum Moench*–Sections  
914 *Eu-sorghum* and *Para-sorghum*. *Grana*, 33, 117–123.

915 Colombaroli, D., Beckmann, M., van der Knaap, W.O., Curdy, P., Tinner, W., 2013. Changes in  
916 biodiversity and vegetation composition in the central Swiss Alps during the transition  
917 from pristine forest to first farming. *Divers. Distrib.* 19, 157–170.

918 Colombaroli, D., Ssemmanda, I., Gelorini, V., Verschuren, D., 2014. Contrasting long-term  
919 records of biomass burning in wet and dry savannas of equatorial East Africa. *Glob.*  
920 *Change Biol.* 20, 2903–2914.

921 Colombaroli, D., Tinner, W., van Leeuwen, J., Noti, R., Vescovi, E., Vanni re, B., Magny, M.,  
922 Schmidt, R., Bugmann, H., 2009. Response of broadleaved evergreen Mediterranean forest  
923 vegetation to fire disturbance during the Holocene: insights from the peri-Adriatic region. *J.*  
924 *Biogeogr.* 36, 314–326.

925 Colombaroli, D., van der Plas, G., Rucina, S., Verschuren, D., 2018. Determinants of savanna-  
926 fire dynamics in the eastern Lake Victoria catchment (western Kenya) during the last 1200  
927 years. *Quatern. Int.* 488, 67–80.

928 Davies, P.T., Tso, M.K-S., 1982. Procedures for reduced-rank regression. *J. Roy. Stat. Soc. C-*  
929 *App.* 31, 244–255.

930 Davies, T.D., Vincent, C.E., Beresford, A.K.C., 1985. July-August rainfall in west-central Kenya.  
931 *J. Climatol.* 5, 17–33.

932 Dearing J.A., Battarbee R.W., Dikau R., Larocque I., Oldfield F., 2006. Human–environment  
933 interactions: learning from the past. *Reg. Environ. Change* 6, 1–16.

934 De Cort, G., Bessems, I., Keppens, E., Mees, F., Cumming, B., Verschuren, D., 2013. Late-  
935 Holocene and recent hydroclimatic variability in the central Kenya Rift Valley: the  
936 sediment record of hypersaline lakes Bogoria, Nakuru and Elementeita. *Palaeogeogr.*  
937 *Palaeoclimatol. Palaeoecol.* 388, 69–80.

938 De Cort, G., Verschuren, D., Ryken, E., Wolff, C., Renaut, R.W., Creutz, M., Van Der Meeren,  
939 T., Haug, G., Olago, D.O., Mees, F., 2018. Multi-basin depositional framework for  
940 moisture-balance reconstruction during the last 1300 years at Lake Bogoria, Central Kenya  
941 Rift Valley. *Sedimentology* 65, 1667–1696.

942 Dickson, C., 1988. Distinguishing cereal from wild grass pollen: some limitations. *Circaea* 5, 67–  
943 71.

944 Dix, N.J., Webster, J., 1995. Coprophilous fungi. In: *Fungal Ecology*. Springer, Dordrecht, pp.  
945 203–224.

946 Driese, S.G., Ashley, G.M., Li, Z.H., Hover, V.C., Owen, R.B., 2004. Possible Late Holocene  
947 equatorial palaeoclimate record based upon soils spanning the Medieval Warm Period and

948 Little Ice Age, Lobo Plain, Kenya. *Palaeogeogr. Palaeoclimatol. Palaeoecol.* 213, 231–  
949 250.

950 Ellis, M.B., 1971. Dematiaceous hyphomycetes. Commonwealth Mycol. Inst., Kew.

951 Eubanks, M., 1997. Reevaluation of the identification of ancient maize pollen from Alabama.  
952 *Am. Antiquity* 62, 139–145.

953 Faegri, K., Iversen, J., 1964. Textbook of pollen analysis. Leiden, The Netherlands.

954 [dataset] FAO, 2015. Food and Agriculture Organization of the United Nations. FAO  
955 GEONETWORK. Land cover of Kenya - Globcover Regional (GeoLayer). (Latest update:  
956 04 Jun 2015) Accessed 18 Sep 2018.

957 Fick, S.E., Hijmans, R.J., 2017. Worldclim 2: New 1-km spatial resolution climate surfaces for  
958 global land areas. *Int. J. Climatol.* 37, 4302–4315.

959 Fuller, D.Q., Hildebrand, E., 2013. Domesticating plants in Africa. In: Mitchell P., Lane P. (Eds),  
960 *The Oxford handbook of African archaeology*. OUP, Oxford, pp. 507–525.

961 Gelorini, V., Ssemmanda, I., Verschuren, D., 2012. Validation of non-pollen palynomorphs as  
962 paleoenvironmental indicators in tropical Africa: contrasting ~200-year paleolimnological  
963 records of climate change and human impact. *Rev. Palaeobot. Palynol.* 186, 90–101.

964 Gelorini, V., Verbeken, A., van Geel, B., Cocquyt, C., Verschuren, D., 2011. Modern non-pollen  
965 palynomorphs from East African lake sediments. *Rev. Palaeobot. Palynol.* 164, 143–173.

966 Goman, M., Ashley, G.M., Owen, R.B., Hover, V.C., Maharjan, D.K., 2017. Late Holocene  
967 Environmental Reconstructions from Lake Solai, Kenya. *Prof. Geogr.* 69, 438–454.

968 Grimm, E.C., 1987. CONISS: a FORTRAN 77 program for stratigraphically constrained cluster  
969 analysis by the method of incremental sum of squares. *Comput. Geosci.* 13, 13–35.

970 Grimm, E., 2015. Tilia and TGView 19 version 2.0. 41. software. Springfield, USA: Illinois State  
971 Museum, Research and Collection Center.

972 Hamilton, A.C., 1972. The interpretation of pollen diagrams from highland Uganda. *Palaeoecol.*  
973 *Afr.* 7, 45–149.

974 Harrison, S.P., Stocker, B.D., Klein Goldewijk, K., Kaplan, J.O., Braconnot, P., 2018. Do we  
975 need to include anthropogenic land-use and land-cover changes in paleoclimate  
976 simulations? *Past Glob. Changes Mag.* 26, 4–5.

977 Heckmann, M., Muiruri, V., Boom, A., Marchant, R., 2014. Human–environment interactions in  
978 an agricultural landscape: A 1400-yr sediment and pollen record from North Pare, NE  
979 Tanzania. *Palaeogeogr. Palaeoclimatol. Palaeoecol.* 406, 49–61.

980 Hildebrand, E.A., Grillo, K.M., Sawchuk, E.A., Pfeiffer, S.K., Conyers, L.B., Goldstein, S.T.,  
981 Hill, A.C., Janzen, A., Klehm, C.E., Helper, M., Kiura, P., 2018. A monumental cemetery  
982 built by eastern Africa’s first herders near Lake Turkana, Kenya. *PNAS* 115, 8942–8947

983 Houghton, R.A., Hackler, J.L., 2006. Emissions of carbon from land use change in sub-Saharan  
984 Africa. *J. Geophys. Res.-Biogeo.* 111(G02003).

985 Johansson, J., Svensson, J., 2002. Land degradation in the semi-arid catchment of Lake Baringo,  
986 Kenya. Report on a minor field study of physical causes with a socio economic aspect.  
987 Department of Geography, University of Goteborg, Sweden.

988 Jolly, D., Taylor, D., Marchant, R., Hamilton, A., Bonnefille, R., Buchet, G., Riollet, G., 1997.  
989 Vegetation dynamics in central Africa since 18,000 yr BP: pollen records from the  
990 interlacustrine highlands of Burundi, Rwanda and western Uganda. *J. Biogeogr.* 24, 492–  
991 512.

992 Kaplan, J.O., Krumhardt, K.M., Ellis, E.C., Ruddiman, W.F., Lemmen, C., Klein Goldewijk, K.,  
993 2011. Holocene carbon emissions as a result of anthropogenic land cover change. *Holocene*  
994 21, 775–791.

995 Kiage, L.M., Liu, K.B., 2009. Palynological evidence of climate change and land degradation in  
996 the Lake Baringo area, Kenya, East Africa, since CE 1650. *Palaeogeogr. Palaeoclimatol.*  
997 *Palaeoecol.* 279, 60–72.

998 Kindt, R., van Breugel, P., Lillesø, J.B., Bingham, M., Demissew, S., Dudley, C., Friis, I.,  
999 Gatchathi F., Kalema, J., Mbago, F., Minani, V., Moshi, H.N., Mulumba, J., Namaganda,  
1000 M., Ndangalasi, H.J., Ruffo, C.K., Jamnadass, R., Graudal, L.O.V., 2011a. Potential  
1001 Natural Vegetation of Eastern Africa (Ethiopia, Kenya, Malawi, Rwanda, Tanzania,  
1002 Uganda and Zambia). Volume 2: Description and Tree Species Composition for Forest  
1003 Potential Natural Vegetation types. Forest, Landscape, University of Copenhagen, Forest,  
1004 Landscape Working Papers, 62.

1005 Kindt, R., van Breugel, P., Lillesø, J.B., Bingham, M., Demissew, S., Dudley, C., Friis, I.,  
1006 Gatchathi F., Kalema, J., Mbago, F., Minani, V., Moshi, H.N., Mulumba, J., Namaganda,  
1007 M., Ndangalasi, H.J., Ruffo, C.K., Jamnadass, R., Graudal, L.O.V., 2011b. Potential  
1008 Natural Vegetation of Eastern Africa (Ethiopia, Kenya, Malawi, Rwanda, Tanzania,  
1009 Uganda and Zambia). Volume 4: Description and Tree Species Composition for Bushland  
1010 and Thicket Potential Natural Vegetation Types. Forest, Landscape, University of  
1011 Copenhagen, Forest, Landscape Working Papers, 64

1012 Klein Goldewijk, K., Beusen, A., van Drecht, G., de Vos, M., 2011. The HYDE 3.1 spatially  
1013 explicit database of human-induced global land-use change over the past 12,000 years.  
1014 *Global Ecol. Biogeogr.* 20, 73–86.

1015 Kokwaro, J.O., 2015. Classification of east African crops. University of Nairobi Press, Nairobi.

1016 Lamb, H., Darbyshire, I., Verschuren, D., 2003. Vegetation response to rainfall variation and  
1017 human impact in central Kenya during the past 1100 years. *Holocene* 13, 285–292.

1018 Lane, P., 2013. Trajectories to pastoralism in northern and central Kenya: an overview of the  
1019 archaeological and environmental evidence. In: Bollig, M., Schnegg, M., Wotza, H.-P.  
1020 (Eds), *Pastoralism in Africa: past, present and future*. Berghahn Books, New York, pp.  
1021 104–144.

1022 Lane, P.J., 2015. Early Agriculture in Sub-Saharan Africa to Ca. AD 500. In: Barker, G.,  
1023 Goucher, C. (Eds), *Cambridge World History, volume 2: A World with Agriculture*.  
1024 Cambridge University Press, Cambridge, pp. 736–773

1025 Lane, P.J., 2016. Entangled banks and the domestication of East African pastoralist landscapes.  
1026 In: Der, L., Fernandini, F. (Eds), *Archaeology of entanglement*, Left Coast Press, Walnut  
1027 Creek, pp. 127–150.

1028 Lewis, S.L., Maslin, M.A., 2015. Defining the Anthropocene. *Nature* 519, 171.

1029 Little, P.D., 1992. The elusive granary: herder, farmer, and state in northern Kenya. Cambridge  
1030 University Press, Cambridge.

1031 Little, P.D., 1996. Pastoralism, biodiversity, and the shaping of savanna landscapes in East  
1032 Africa. *Africa* 66, 37–51.

1033 Marchant, R., Richer, S., Boles, O., Capitani, C., Courtney-Mustaphi, C., Lane, P., Prendergast,  
1034 M., Stump, D., De Cort, G., Kaplan, J.O., Phelps, L., Kay, A., Olago, D., Petek, N., Platts,  
1035 P.J., Punwong, P., Widgren, M., Wynne-Jones, S., Ferro-Vázquez, C., Benard, J., Boivin,  
1036 N., Crowther, A., Cuní-Sanchez, A., Deere, N.J., Ekblom, A., Farmer, J., Finch, J., Fuller,  
1037 D., Gaillard-Lemdahl, M.-J., Gillson, L., Githumbi, E., Kabora, T., Kariuki, R., Kinyanjui,  
1038 R., Kyazike, E., Lang, C., Lejju, J., Morrison, K.D., Muiruri, V., Mumbi, C., Muthoni, R.,  
1039 Muzuka, A., Ndiema, E., Nzabandora, C.K., Onjala, I., Schrijver, A.P., Rucina, S.,  
1040 Shoemaker, A., Thornton-Barnett, S., van der Plas, G., Watson, E.E., Williamson, D.,

1041 Wright, D., 2018. Drivers and trajectories of land cover change in East Africa: Human and  
1042 environmental interactions from 6000 years ago to present. *Earth-Sci. Rev.* 178, 322–378.

1043 Marlon, J., Bartlein, P., Carcaillet, C., Gavin, D.G., Harrison, S.P., Higuera, P.E., Joos, F.,  
1044 Power, M.J., Prentice, C.I., 2008. Climate and human influences on global biomass burning  
1045 over the past two millennia. *Nat. Geosci.* 1, 697–701.

1046 Marshall, F., Hildebrand, E., 2002. Cattle before crops: the beginnings of food production in  
1047 Africa. *J. World Prehist.* 16, 99–143.

1048 Moore, P.D., Webb, J.A., 1978. *Illustrated guide to pollen analysis*. Hodder and Stoughton,  
1049 London.

1050 Moore, P.D., Webb, J.A., Collison, M.E., 1991. *Pollen analysis*. Blackwell scientific  
1051 publications, Oxford.

1052 Mwangi, E., Swallow, B., 2008. *Prosopis juliflora* invasion and rural livelihoods in the Lake  
1053 Baringo Area of Kenya. *Conserv. Soc.* 6: 130–140.

1054 [dataset] NASA LP DAAC (2011). ASTER Global Digital Elevation Model, version 2. NASA  
1055 EOSDIS Land Processes DAAC, USGS Earth Resources Observation and Science (EROS)  
1056 Center, Sioux Falls, South Dakota (<https://lpdaac.usgs.gov>), accessed 2018.

1057 Nash, D.J., Pribyl, K., Klein, J., Neukom, R., Endfield, G.H., Adamson, G.C., Kniveton, D.R.,  
1058 2016. Seasonal rainfall variability in southeast Africa during the nineteenth century  
1059 reconstructed from documentary sources. *Climatic change* 134, 605–619.

1060 Nicholson, S.E., 1996. A review of climate dynamics and climate variability in Eastern Africa.  
1061 In: Johnson, T.C., Odada, E.O. (Eds.), *The Limnology, Climatology and Paleoclimatology*  
1062 *of the East African Lakes*. Gordon and Breach, Amsterdam, pp. 25–56.

1063 Nicholson, S.E., 2018. The ITCZ and the seasonal cycle over equatorial Africa. *B. Am. Meteorol.*  
1064 *Soc.* 99, 337–348.

- 1065 Ofcansky, T.P., 1984. Kenya forestry under British colonial administration, 1895-1963. *J. For.*  
1066 *Hist.* 28, 136–143.
- 1067 Onyando, J.O., Musila, F., Awer, M., 2005. The use of GIS and remote sensing techniques to  
1068 analyse water balance of Lake Bogoria under limited data conditions. *J. Civ. Eng. Res.*  
1069 *Pract.* 2, 53–65.
- 1070 Petek, N., 2018. Archaeological Perspectives on Risk and Community Resilience in the Baringo  
1071 Lowlands, Kenya. Unpublished thesis, Department of Archaeology and Ancient History,  
1072 Uppsala University.
- 1073 Petek, N., Lane, P., 2017. Ethnogenesis and surplus food production: communitas and identity  
1074 building among nineteenth-and early twentieth-century Ilchamus, Lake Baringo, Kenya.  
1075 *World Archaeol.* 49, 40–60.
- 1076 Prentice, I.C., 1985. Pollen representation, source area, and basin size: toward a unified theory of  
1077 pollen analysis. *Quat. Res.* 23, 76–86.
- 1078 Prentice, I.C., Webb III, T., 1986. Pollen percentages, tree abundances and the Fagerlind effect. *J.*  
1079 *Quat. Sci.* 1, 35–43.
- 1080 Ramankutty, N., Foley, J.A., 1999. Estimating historical changes in global land cover: Croplands  
1081 from 1700 to 1992. *Global Biogeochem. Cy.* 13, 997–1027.
- 1082 Reimer, P.J., Bard, E., Bayliss, A., Beck, J.W., Blackwell, P.G., Ramsey, C.B., Buck, C.E.,  
1083 Cheng, H., Edwards, R.L., Friedrich, M., Grootes, P.M., 2013. IntCal13 and Marine13  
1084 radiocarbon age calibration curves 0–50,000 years cal BP. *Radiocarbon* 55, 1869–1887.
- 1085 Renaut, R.W., Tiercelin, J.-J., 1994. Lake Bogoria, Kenya Rift Valley: a sedimentological  
1086 overview. In: Renaut R.W., Last W.M. (Eds), *Sedimentology and Geochemistry of Modern*  
1087 *and Ancient Saline Lakes. Soc. Econ. Paleont. Mineral. Spec. Publ.* 50, 101–123.

- 1088 Renaut, R.W., Tiercelin, J.-J., Owen, R.B., 1986. Mineral precipitation and diagenesis in the  
1089 sediments of the Lake Bogoria basin, Kenya Rift Valley. In: Frostick, L.E., Renaut, R.W.,  
1090 Reid I., Tiercelin J.-J. (Eds), Sedimentation in the African Rifts. Geol. Soc. Lond. Spec.  
1091 Publ. 25, 159–175.
- 1092 Shoemaker, R.A., 1959. Nomenclature of Drechslera and Bipolaris, grass parasites segregated  
1093 from ‘Helminthosporium’. Can. J. Botany 37, 879–887.
- 1094 Schüler, L., Hemp, A., 2016. Atlas of pollen and spores and their parent taxa of Mt Kilimanjaro  
1095 and tropical East Africa. Quatern. Int. 425, 301–386.
- 1096 Ssemmanda, I., Gelorini, V., Verschuren, D., 2014. Sensitivity of the grassland-forest ecotone in  
1097 East African open woodland savanna to historical rainfall variation. Clim. Past 10, 2067–  
1098 2080.
- 1099 Stocker, B.D., Yu, Z., Joos, F., 2018. Contrasting CO<sub>2</sub> emissions from different Holocene land-  
1100 use reconstructions: Does the carbon budget add up? Past Glob. Changes Mag. 26, 6–7.
- 1101 Taylor, D.M., 1990. Late quaternary pollen records from two Ugandan mires: evidence for  
1102 environmental changes in the Rukiga highlands of southwest Uganda. Palaeogeogr.  
1103 Palaeoclimatol. Palaeoecol. 80, 283–300.
- 1104 Taylor, D., Marchant, R.A., Robertshaw, P., 1999. A sediment-based history of medium altitude  
1105 forest in central Africa: a record from Kabata Swamp, Ndale volcanic field, Uganda. J.  
1106 Ecol. 87, 303–315.
- 1107 Taylor, D., Lane, P.J., Muiruri, V., Ruttledge, A., McKeever, R.G., Nolan, T., Kenny, P.,  
1108 Goodhue, R., 2005. Mid-to late-Holocene vegetation dynamics on the Laikipia Plateau,  
1109 Kenya. Holocene 15, 837–846.
- 1110 Ter Braak, C.J., 1988. CANOCO – a FORTRAN program for canonical community ordination  
1111 by [partial][detrended][canonical] correspondence analysis, principal components analysis

- 1112 and redundancy analysis (version 2.1) Report LWA-88-02. Agricultural Mathematics  
1113 Group, Wageningen.
- 1114 Ter Braak, C.J., Prentice, I.C., 1988. A theory of gradient analysis. *Adv. Ecol. Res.* 18, 271–317.
- 1115 Tierney, J.E., Smerdon, J.E., Anchukaitis, K.J., Seager, R., 2013. Multidecadal variability in East  
1116 African hydroclimate controlled by the Indian Ocean. *Nature*, 493, 389.
- 1117 Troup, R. S., 1932. *Exotic forest trees in the British Empire*. Clarendon Press, Oxford.
- 1118 Tsukada, M., Rowley, J.R., 1964. Identification of modern and fossil maize pollen. *Grana*, 5,  
1119 406–412.
- 1120 van Breugel, P., Kindt, R., Lillesø, J.P.B., Bingham, M., Demissew, S., Dudley, C., Friis, I.,  
1121 Gatchathi F., Kalema, J., Mbago, F., Moshi, H.N., Mulumba, J.W., Namaganda, M.,  
1122 Ndangalasi, H.J., Ruffo, C.K., Minani, V., Jamnadass, R., Gaudal, L., 2015. Potential  
1123 Natural Vegetation Map of Eastern Africa (Burundi, Ethiopia, Kenya Malawi, Rwanda,  
1124 Tanzania, Uganda and Zambia). Version 2.0.
- 1125 van Geel, B., Buurman, J., Brinkkemper, O., Schelvis, J., Aptroot, A., van Reenen, G., Hakbijl,  
1126 T., 2003. Environmental reconstruction of a Roman Period settlement site in Uitgeest (The  
1127 Netherlands), with special reference to coprophilous fungi. *J. Archaeol. Sci.* 30, 873–883.
- 1128 van Geel, B., Coope, G. R., van der Hammen, T., 1989. Palaeoecology and stratigraphy of the  
1129 Lateglacial type section at Usselo (The Netherlands). *Rev. Palaeobot. Palynol.* 60, 25–129.
- 1130 van Geel, B., Gelorini, V., Lyaruu, A., Aptroot, A., Rucina, S., Marchant, R., Damsté, J.S.S.,  
1131 Verschuren, D., 2011. Diversity and ecology of tropical African fungal spores from a  
1132 25,000-year palaeoenvironmental record in southeastern Kenya. *Rev. Palaeobot. Palynol.*  
1133 164, 174–190.
- 1134 Vehrs, H.P., 2016. Changes in landscape vegetation, forage plant composition and herding  
1135 structure in the pastoralist livelihoods of East Pokot, Kenya. *J. East. Afr. Stud.* 10, 88–110.

- 1136 Vehrs, H.P., Heller, G.R., 2017. Fauna, Fire, and Farming: Landscape Formation over the Past  
1137 200 years in Pastoral East Pokot, Kenya. *Hum. Ecol.* 45, 613–625.
- 1138 Verschuren, D., 1999. Sedimentation controls on the preservation and time resolution of climate-  
1139 proxy records from shallow fluctuating lakes. *Quat. Sci. Rev.* 18, 821–837.
- 1140 Verschuren, D., 2001. Reconstructing fluctuations of a shallow East African lake during the past  
1141 1800 yrs from sediment stratigraphy in a submerged crater basin. *J. Paleolimnol.* 25, 297–  
1142 311.
- 1143 Verschuren, D., 2003. Lake-based climate reconstruction in Africa: progress and challenges.  
1144 *Hydrobiologia* 500, 315–330.
- 1145 Verschuren, D. (2004). Decadal and century-scale climate variability in tropical Africa during the  
1146 past 2000 years. *Dev. Paleoenviron. Res.* 6, 139-158.
- 1147 Verschuren, D., Charman, D.J. 2008. Latitudinal linkages in late Holocene moisture-balance  
1148 variation. In: Battarbee, R.W., Binney, H.A. (Eds.), *Natural climate variability and global  
1149 warming: a Holocene perspective.* Wiley-Blackwell, Chichester, pp.189–231.
- 1150 Verschuren, D., Laird, K.R., Cumming, B.F., 2000. Rainfall and drought in equatorial east Africa  
1151 during the past 1,100 years. *Nature* 403, 410.
- 1152 Verschuren, D., Tibby, J., Leavitt, P.R., Roberts, C.N., 1999. The environmental history of a  
1153 climate-sensitive lake in the former 'White Highlands' of central Kenya. *Ambio* 28, 494–  
1154 501.
- 1155 Vincens, A., 1986. Diagramme pollinique d'un sondage Pleistocene superieur—Holocene du Lac  
1156 Bogoria (Kenya). *Rev. Palaeobot. Palynol.* 47, 169–192.
- 1157 Vincens, A., Bremond, L., Brewer, S., Buchet, G., Dussouillez, P., 2006. Modern pollen-based  
1158 biome reconstructions in East Africa expanded to southern Tanzania. *Rev. Palaeobot.  
1159 Palynol.* 140, 187–212.

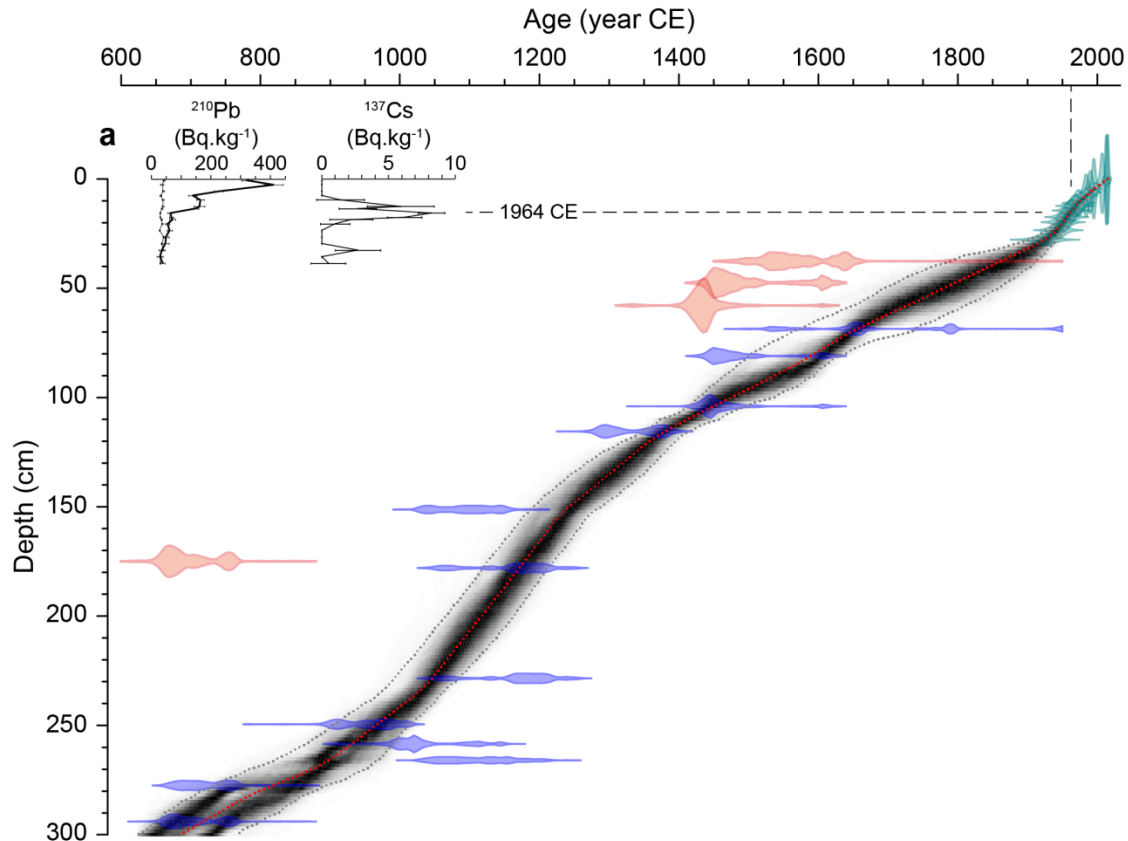
- 1160 Vincens, A., Casanova, J., Tiercelin, J.J., 1986. Palaeolimnology of Lake Bogoria (Kenya) during  
1161 the 4500 BP high lacustrine phase. In: Frostick, L.E., Renaut, R.W., Reid I., Tiercelin J.-J.  
1162 (Eds), Sedimentation in the African Rifts. Geol. Soc. Lond. Spec. Publ. 25, 323–330.
- 1163 White, F., 1983. The vegetation of Africa: a descriptive memoir to accompany the  
1164 UNESCO/AETFAT/UNSO vegetation map of Africa by F White. Natural Resources  
1165 Research Report XX, UNESCO, Paris, France.
- 1166 Widgren, M., Sutton, J.E., 2004. Islands of intensive agriculture in Eastern Africa: past, present.  
1167 James Currey Publishers, Oxford.
- 1168 Yang, W., Seager, R., Cane, M.A., Lyon, B., 2015. The annual cycle of East African  
1169 precipitation. *J. Clim.* 28, 2385–2404.
- 1170

1171 **Distinct phases of natural landscape dynamics and intensifying human activity**  
1172 **in the central Kenya Rift Valley during the past 1300 years**

1173 G. W. van der Plas, G. De Cort, N. Petek-Sargeant, T. Wuytack, D. Colombaroli, P. J. Lane, D.  
1174 Verschuren

1175 **SUPPLEMENTARY INFORMATION**

1176 **1. Sediment sampling and chronology** (supplement to section 3.1)



1177  
1178 **Fig. S1** Age–depth model for composite core BOGS14 from the southern basin of Lake Bogoria,  
1179 generated with the Bacon software package for R (Blaauw & Christen, 2011). ‘Mirrored’  
1180 calendar-age distributions, with height proportional to probability, are shown for both  $^{210}\text{Pb}$ -  
1181 derived ages (green) and  $^{14}\text{C}$ -dated intervals (blue if incorporated in the age model; pink if not  
1182 retained). The 12 incorporated  $^{14}\text{C}$  dates infer realistic changes in age with depth, even in core  
1183 sections with syn-sedimentary growth of large nahcolite crystals (255-210 cm depth) or high  
1184 rates of clastic sediment input. The red dotted line depicts the modelled age–depth relationship  
1185 (weighted mean of model iterations), with grey dotted lines indicating the upper and lower  
1186 boundaries of the 95% confidence interval. Insert plots show the depth profile of total (thick line)  
1187 and supported (thin line)  $^{210}\text{Pb}$  activity in the uppermost sediments, as well as  $^{137}\text{Cs}$  activity  
1188 which displays a peak at AD 1964. Modified from De Cort et al., (2018).

1189 **2. Pollen and fungal-spore analysis** (supplement to section 3. 2)

1190 Raw sediment was treated with hydrochloric acid, warm 10% potassium hydroxide, 96% acetic  
1191 acid, and an acetolysis mixture of 1:9 sulphuric acid and acetic anhydride boiled to 100 °C.  
1192 Heavy liquid separation using sodium polytungstate with a specific gravity of 2.0 was used to  
1193 separate the pollen from mineral components. For pollen identification, we referred to  
1194 photographs of voucher specimens in standard atlases (Bonnefille & Riollet, 1980; Schüler &  
1195 Hemp, 2016); our nomenclature follows the African Pollen Database (Vincens et al., 2007).  
1196 Slides from BOGS14 were most often counted completely. After reaching the desired pollen sum  
1197 in BOGN14 slides, the remainder of the slides was scanned for rare plant taxa to confirm their  
1198 presence or absence in that particular time window. Pollen preservation was generally good to  
1199 excellent, with the exception of a short section of BOGN14 covering four sampling intervals  
1200 (125.5-126.5, 128-129, 131-132, 137.5-138.5 cm composite depth), where sample processing  
1201 proved problematic and the resulting pollen count was atypically low (with a minimum of only  
1202 111 grains at 131-132 cm depth). Because of these difficulties, fungal-spore counts in these  
1203 intervals required correction through additional pollen analysis. This correction was not possible  
1204 for fungal spore taxa with only sporadic appearances, and hence these rare taxa were omitted  
1205 from the BOGN14 diagram (Fig. 6).

1206 Besides being more or less continuously present in Lake Bogoria sediments dated to the  
1207 last *ca* 70 years, a few *Pinus*-type pollen grains were also recovered from isolated core intervals  
1208 dated to *ca* 1800 CE in BOGS14, and *ca* 1850 CE in BOGN14. Although pine trees have been  
1209 planted in South Africa since the early 18<sup>th</sup> century (Burgess & Wingfield, 2001), there is no  
1210 record of pine being present in East Africa before the early 20<sup>th</sup> century. Considering the methods  
1211 of core collection and processing (De Cort et al., 2018) and the permanently anoxic bottom  
1212 environment of Lake Bogoria (translated in the sediments being finely laminated), we can  
1213 exclude the possibility of cross-level contamination or post-depositional movement of pollen  
1214 grains through the sequence. We therefore treated these old *Pinus*-type grains as aberrant  
1215 *Podocarpus* pollen, and excluded them from all analyses.

1216 **3. Landscape history as recorded in the southern basin of Lake Bogoria** (suppl. to section 4.  
1217 1)

1218 *Zone BOGS-1 (ca 700 – 1175 CE)*. The grass pollen fraction is relatively high (Fig. 2),  
1219 fluctuating around 50% with two pronounced but short-lived dips around 960 CE (38%) and  
1220 1130 CE (31%). The Afromontane forest component is substantial (26-39%, mean 30%) and  
1221 dominated by *Podocarpus*, *Olea* and Cupressaceae (at that time, *Juniperus procera*). The  
1222 decrease in Cupressaceae and increase in *Olea* around 900 CE drives the division of this zone in  
1223 sub-zones BOGS-1a and BOGS-1b. The smaller woodland fraction (9-25%, mean 16%) is  
1224 relatively stable through time and consists primarily of *Acalypha* with smaller contributions from  
1225 Combretaceae, *Dodonaea*, *Euphorbia* (mostly *E. cf. acalyphoides*) and *Acacia*. Also the  
1226 herbaceous component is relatively modest (3-9%, mean 6%). On the whole the pollen

1227 assemblage indicates that much of the catchment was covered by relatively open grassland-  
1228 woodland ecotonal vegetation, with stands of closed-canopy forest relatively nearby.

1229 *Zone BOGS-2 (ca 1175 – 1330 CE)*. Grass pollen (22-40%) decreases to levels well below those  
1230 in BOGS-1 during two multi-decadal episodes centered around 1220 CE (22%) and 1280 CE  
1231 (30%). The compensation by other elements of the vegetation, however, differs between the two  
1232 episodes, resulting in a division into sub-zones BOGS-2a (1175 – 1250 CE) and BOGS-2b (1250  
1233 – 1330 CE). BOGS-2a is characterized by an increase of the forest component (36-54%, mean  
1234 38%) carried in large part by *Olea* (up to 39%). In BOGS-2b there are major increases in *Justicia*  
1235 spp., *Acacia*, Asteraceae and Amaranthaceae, which are all trees and herbs associated with  
1236 *Acacia* wooded grassland (Vincens et al., 2006). However, one characteristic woodland shrub  
1237 with generally reduced prominence throughout BOGS-2, compared to BOGS-1, is *Acalypha*.  
1238 Overall the woodland fraction varies between 14-22% (mean 17%) in BOGS-2a and 10-26%  
1239 (mean 15%) in BOGS-2b. The forest component in BOGS-2b ranges between 22 and 40% (mean  
1240 29%), i.e. similar to the situation in BOGS-1.

1241 *Zone BOGS-3 (ca 1330 – 1430 CE)*. Grass pollen percentages increase again, reaching 46-53%  
1242 within this zone. The taxa associated with *Acacia*-wooded grassland decrease again, but this is  
1243 largely compensated by re-expansion of *Acalypha*. The total woodland (10-18%, mean 13%) and  
1244 forest (27-31%, mean 28%) fractions remained mostly constant relative to BOGS-2b, and in the  
1245 latter *Olea* and *Podocarpus* remain prominent at mean values of 20% and 12%.

1246 *Zone BOGS-4 (ca 1430 – 1910 CE)*. This pollen zone encompasses a *ca* 500-year period of Rift  
1247 Valley history, ending in the early 20th century. Grasses are abundant throughout most of this  
1248 period, with percentages mostly exceeding 60% and reaching peak values of 75-76% around  
1249 1710 CE and 1840 CE. After this most recent peak, Poaceae decrease again to *ca* 50% at the top  
1250 of this zone. In the forest component, *Olea* can maintain its 20% level only until *ca* 1500 CE,  
1251 after which it decreases mostly to the benefit of Cupressaceae. From *ca* 1500 CE, Poaceae grains  
1252 in the size range 60–85  $\mu\text{m}$  start appearing more or less continuously and in significant numbers,  
1253 although they were occasionally present already in BOGS-1 and BOGS-3 (but not in BOGS-2).  
1254 Also cf. *Ricinus* (castor oil plant), previously showing only erratic occurrences, makes more  
1255 regular appearances from *ca* 1600 AD onwards although it remains rare (Fig. 2). Although this  
1256 500-year period is delineated as a single zone by CONISS, by no means vegetation composition  
1257 in the southern Bogoria catchment (and beyond) remained stable throughout. Marked percent-  
1258 abundance shifts are more or less concentrated around 1670 CE, resulting in a division between  
1259 sub-zones BOGS-4a and BOGS-4b at that level. In the forest, cf. *Calodendrum* and *Hagenia*  
1260 decreased to the benefit of *Artemisia*; in the woodland, *Dodonaea* decreased to the benefit of  
1261 *Justicia* and *Euphorbia*. Other woodland trees such as *Acacia* and Combretaceae maintain  
1262 relatively stable populations throughout BOGS-4. Overall, however, the total woodland  
1263 component was strongly reduced, with a mean low value of 6% between *ca* 1480 and 1870 CE  
1264 (Fig. 2). Meanwhile *Podocarpus* mostly maintains stable values of *ca* 15%, falling to values  
1265 consistently <10% only between *ca* 1700 and 1780 CE. Coincidence with low *Olea* abundance

1266 around the start of this period reduces the total Afromontane forest component to less than 20%  
1267 around 1700 CE, its lowest level of the entire record.

1268 *Zone BOGS-5 (ca 1910 – 1965 CE)*. During this period, which broadly encompasses the period  
1269 of European colonial rule, Poaceae pollen decreased further to reach a low value of *ca* 30%  
1270 around 1960 CE. The wooded savanna arboreal taxa *Acacia*, Combretaceae, *Justicia* spp., cf.  
1271 *Dobera/Nuxia* and *Euclea* all increase, realizing a recovery of the woodland component to 8-17%  
1272 (in the case of *Euclea*, expansion had already started in the upper part of BOGS-4). This  
1273 woodland recovery is also reflected in marked increases of herbaceous taxa belonging to the  
1274 Amaranthaceae and Asteraceae. Other herbaceous taxa that increase are cf. *Ricinus* and *Tribulus*,  
1275 and diverse rare taxa such as cf. *Corchorus*, cf. *Hypoestes*, unidentified Loranthaceae and  
1276 Malvaceae. The Afromontane forest component expands (to a peak value of 40%) only  
1277 temporarily in the lower part of this zone, representing the early 20th century. Notably, whereas  
1278 the previous episode of forest expansion (in BOGS-2) was mostly on account of *Olea*,  
1279 Afromontane taxa that increase now are the Cupressaceae, *Artemisia*, *Croton*, *Hagenia* and  
1280 *Myrica*. No Poaceae grains >60  $\mu\text{m}$  (either 60–85  $\mu\text{m}$  or >85  $\mu\text{m}$ ) were recovered from this  
1281 pollen zone.

1282 *Zone BOGS-6 (ca 1965 – 2014 CE)*. This most recent period, which broadly encompasses the  
1283 post-colonial period, sees the fraction of Poaceae pollen decline further still to reach its lowest  
1284 value of the entire record (18%) in the pollen assemblage representing modern-day vegetation.  
1285 This is not only due to the strong Afromontane (38-46%) and Herbaceous (9-16%) components  
1286 but also the relatively high values (14-25%) for Woodland (due to unprecedented increases in  
1287 *Dodonaea* and *Syzygium*), and appearance of the exotic cultivar *Pinus*. Likely, the unprecedented  
1288 increase in Cupressaceae in this zone must be attributed largely to the planting of exotic cypress  
1289 species for timber production. Noteworthy herbs include *Plantago*, cf. *Ricinus*, cf. *Corchorus* and  
1290 cf. *Hypoestes*. Only a single Poaceae grain >85  $\mu\text{m}$  (maize) was recovered from BOGS-6, and  
1291 none in the 60-85  $\mu\text{m}$  range.

#### 1292 **4. Additional reference**

1293 Vincens, A., Lézine, A. M., Buchet, G., Lewden, D., Le Thomas, A., 2007. African pollen  
1294 database inventory of tree and shrub pollen types. *Rev. Palaeobot. Palynol.* 145, 135–141.  
1295

1296 **Figure captions**

1297  
1298 **Fig. 3** (a) Location of Lake Bogoria, its drainage basin (bold line), major rivers feeding into the  
1299 lake (thin lines) and the Lake Bogoria National Reserve (boundary as stippled line), in relation to  
1300 other regional lakes and surrounding topography. Topography data are from the Advanced  
1301 Spaceborne Thermal Emission and Reflection Radiometer (ASTER) Global Digital Elevation  
1302 Model (GDEM) data set (NASA LP DAAC, 2011). (b) Potential vegetation of the study region,  
1303 simplified from the VECEA classification (van Breugel et al., 2015). Superimposed on this map  
1304 are the isolines of mean annual rainfall for the period 1970-2000 based on the Worldclim 2.0  
1305 dataset (Fick & Hijmans, 2017) shown to highlight the moisture dependence of vegetation  
1306 distribution. (c) Map of current land cover and land use, derived from Globcover data for 2009  
1307 (Bontemps, 2011) using a regional model by the Food and Agriculture Organization of the  
1308 United Nations (FAO, 2015). The skeleton map shows the location of the study area in eastern  
1309 equatorial Africa.

1310  
1311 **Fig. 4** Stratigraphic distribution of selected pollen taxa (most, but not all >1% of the terrestrial  
1312 pollen sum) in the BOGS14 sediment sequence from the southern basin of Lake Bogoria, in  
1313 relation to sediment age (De Cort et al., 2018) and pollen-based stratigraphic zonation (CONISS;  
1314 Grimm, 1987). Taxon abundance is presented as percentage (%) of the terrestrial pollen sum  
1315 (black curves; 10x exaggeration in white), with taxa grouped per vegetation type and summary  
1316 diagram on the left. Pollen from wetland taxa and fungal spores are expressed as percent of the  
1317 terrestrial pollen sum but not included in it.

1318  
1319 **Fig. 3** Synthesis of proxy data from the southern (BOGS14, green) and northern (BOGN14, blue)  
1320 sediment record of Lake Bogoria, with indication of the five phases of intensifying ecological  
1321 influence of human activity (light to dark grey shading). The panels show (a) climatic moisture-  
1322 balance variation inferred from lake-level change, simplified from De Cort et al. (2018); (b) clay  
1323 fraction as % of clastic mineral sediment; (c) total lake-sediment accumulation rate (SAR); (d)  
1324 biomass burning inferred from charcoal influx; (e) cereal production inferred from the fraction of  
1325 Poaceae pollen grains sized 60-85  $\mu\text{m}$ , with isolated finds of maize pollen (Poaceae grains >85  
1326  $\mu\text{m}$ ) indicated with pictograms; (f) Animal husbandry (plus wild herbivores; see text), inferred  
1327 from the relative abundance of spores from obligate coprophilous fungi (*Sporormiella* +  
1328 *Sordaria*); (g) summary diagram of temporal shifts in the composition of terrestrial vegetation,  
1329 based on BOGS14 data.

1330  
1331 **Fig. 4** Percentage (%) of 60-85  $\mu\text{m}$  Poaceae pollen grains versus the total % abundance of  
1332 Poaceae pollen, with symbol colors representing the successive pollen zones. Also shown are the  
1333 linear regression for all pollen zones (black line), and the average values ( $\pm$  SE) of each pollen  
1334 zone separately (colored crosses).

1335

1336 **Fig. 5** Principal Component Analysis (PCA) of the temporal distribution of pollen taxa in  
1337 sediment sequence BOGS14. (a) Species plot with color coding according to vegetation type, as  
1338 in Fig. 2. (b) Sample plot with samples labelled by age, and grouped using colored polygons to  
1339 demarcate the pollen zones, as in Fig. 3.

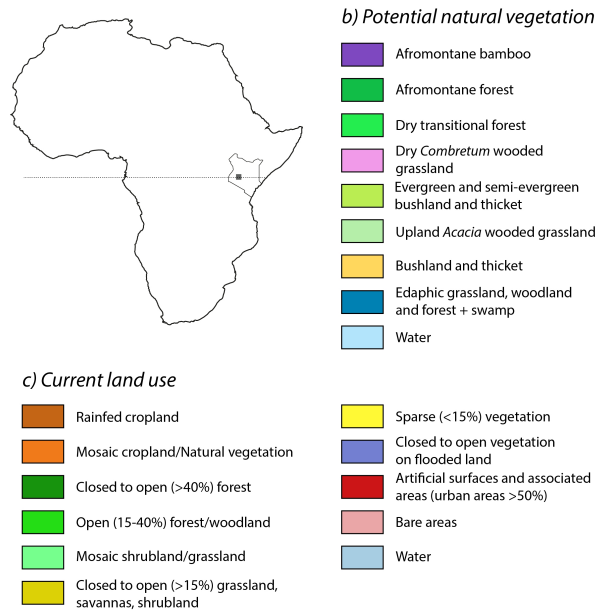
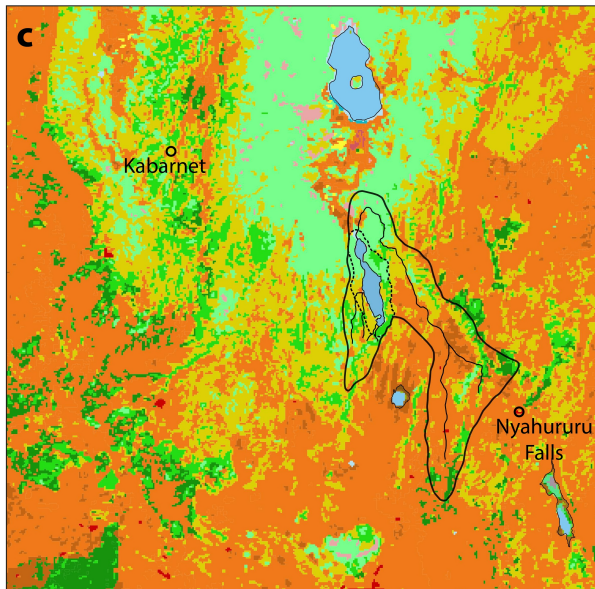
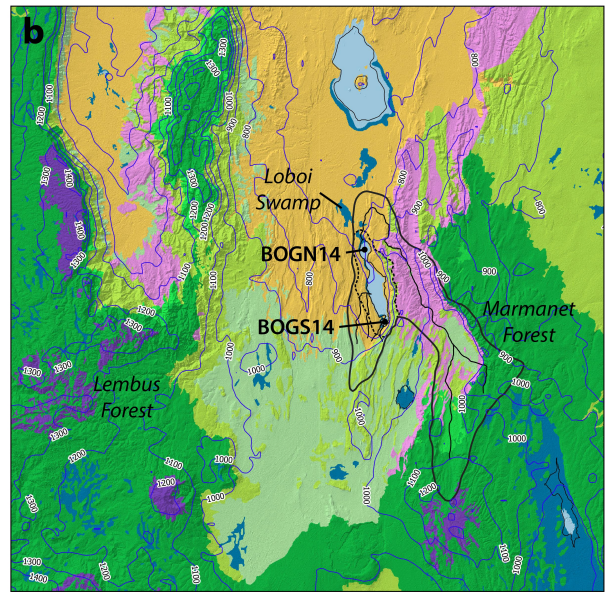
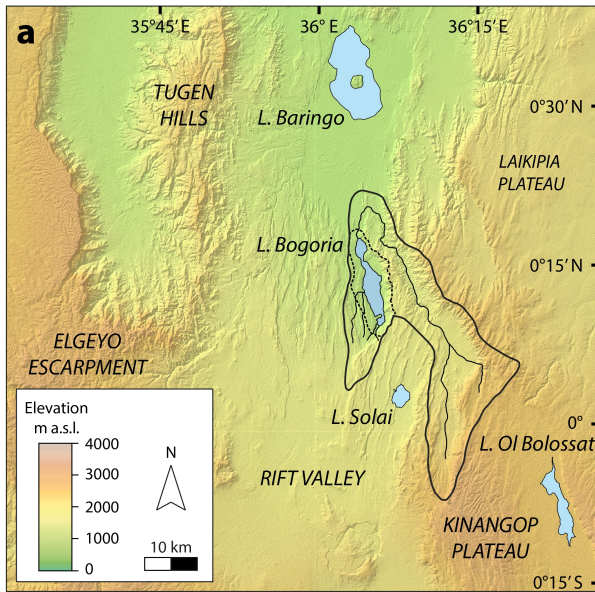
1340  
1341 **Fig. 6** Stratigraphic distribution of selected pollen taxa (all >1% of the terrestrial pollen sum) in  
1342 the BOGN14 sediment sequence from the northern basin of Lake Bogoria, in relation to sediment  
1343 age (De Cort et al., 2018) and pollen-based stratigraphic zonation (CONISS; Grimm, 1987).  
1344 Taxon abundance is presented as percentage (%) based on the terrestrial pollen sum (black  
1345 curves; 10x exaggeration in white), with taxa grouped per vegetation type. A summary diagram is  
1346 shown on the left. Pollen from wetland taxa and fungal spores are expressed as percent of the  
1347 terrestrial pollen sum but not included in it.

1348

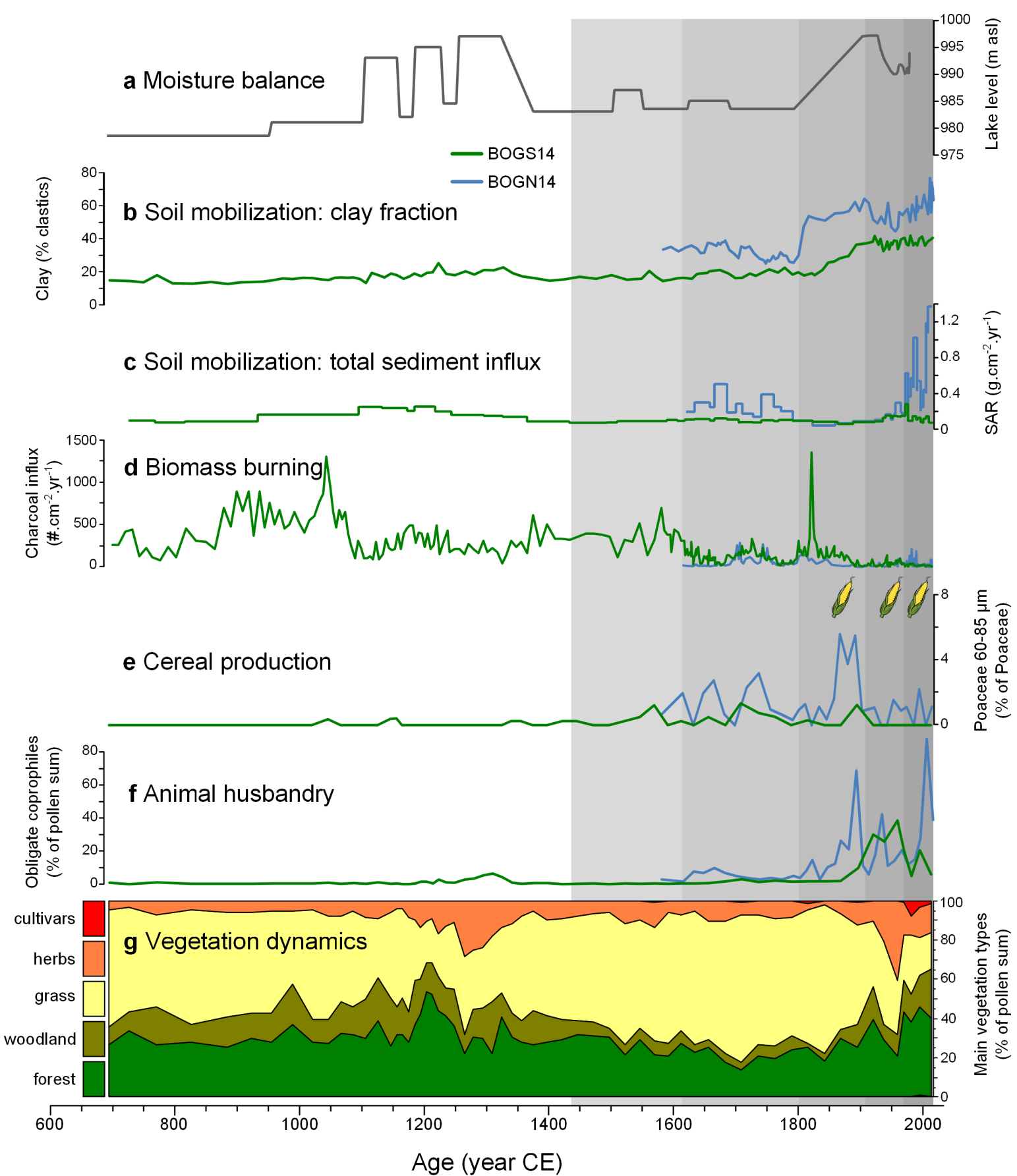
1349 **Table captions**

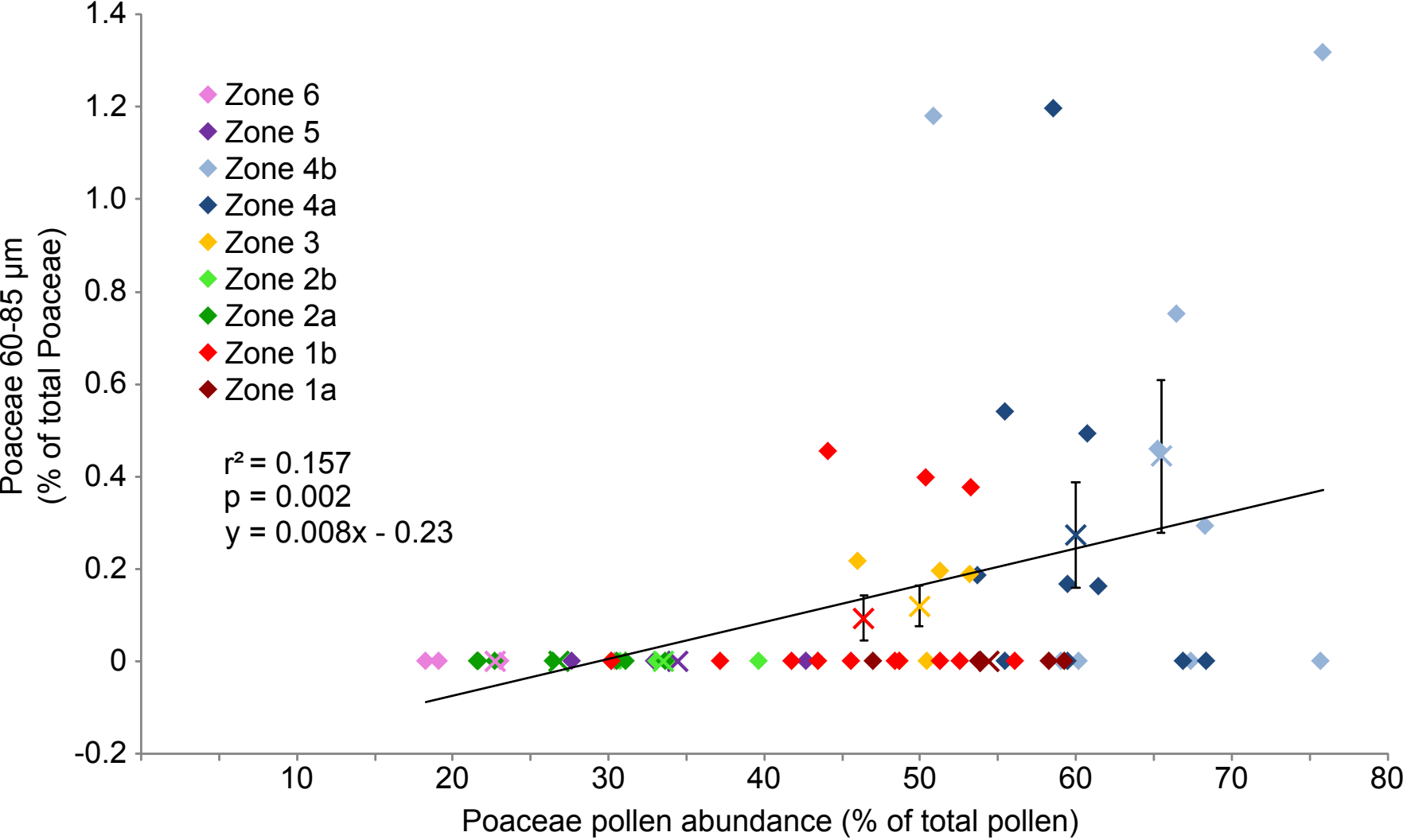
1350

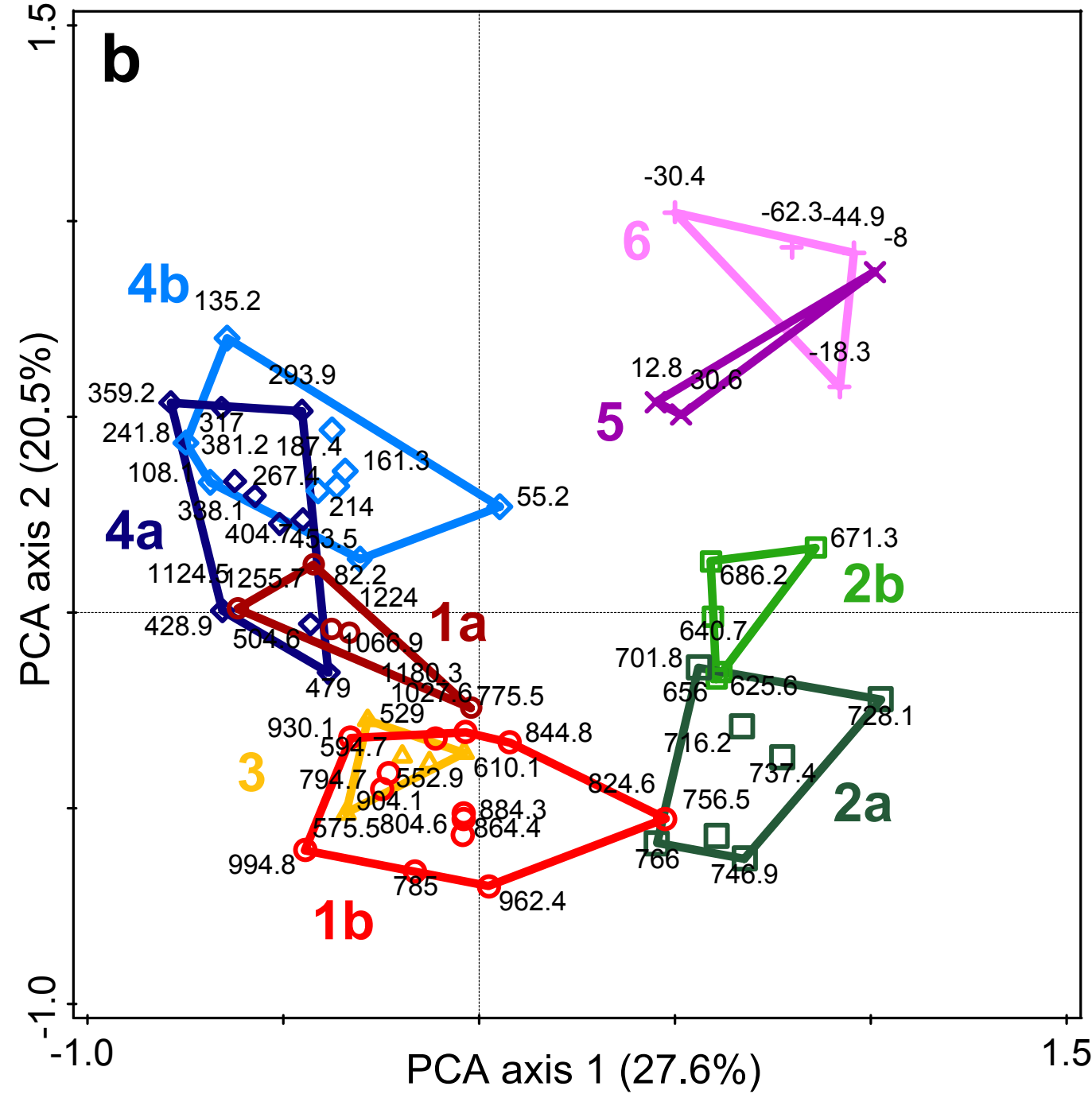
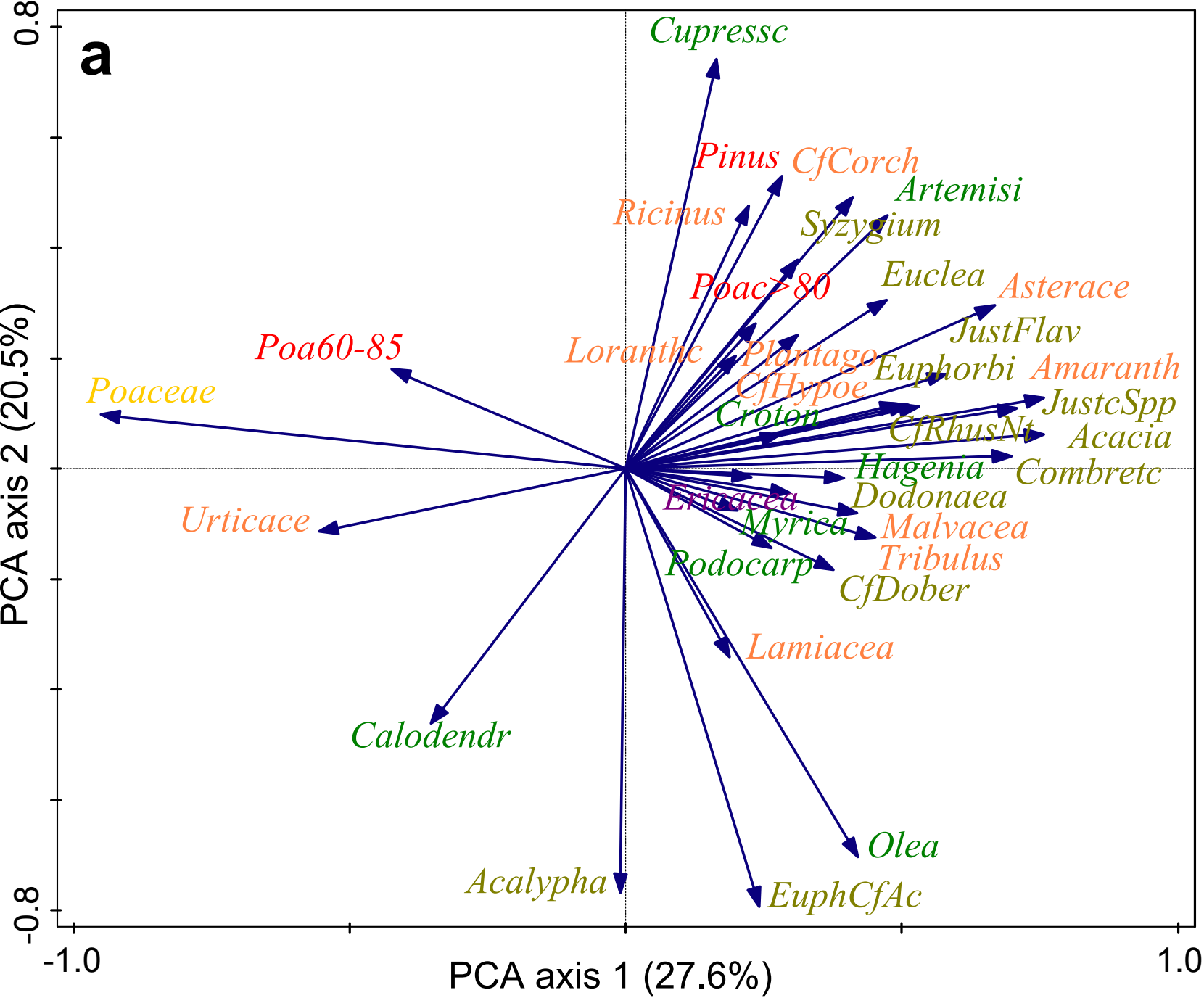
1351 **Table 2** Sediment depth, weighted-mean modelled age and the lower and upper boundaries of  
1352 95% confidence envelopes (Min/Max Age) of pollen-zone boundaries in composite sequence  
1353 BOGS14 from the southern basin of Lake Bogoria, based on  $^{210}\text{Pb}$ - and  $^{14}\text{C}$ -dating by De Cort et  
1354 al. (2018).

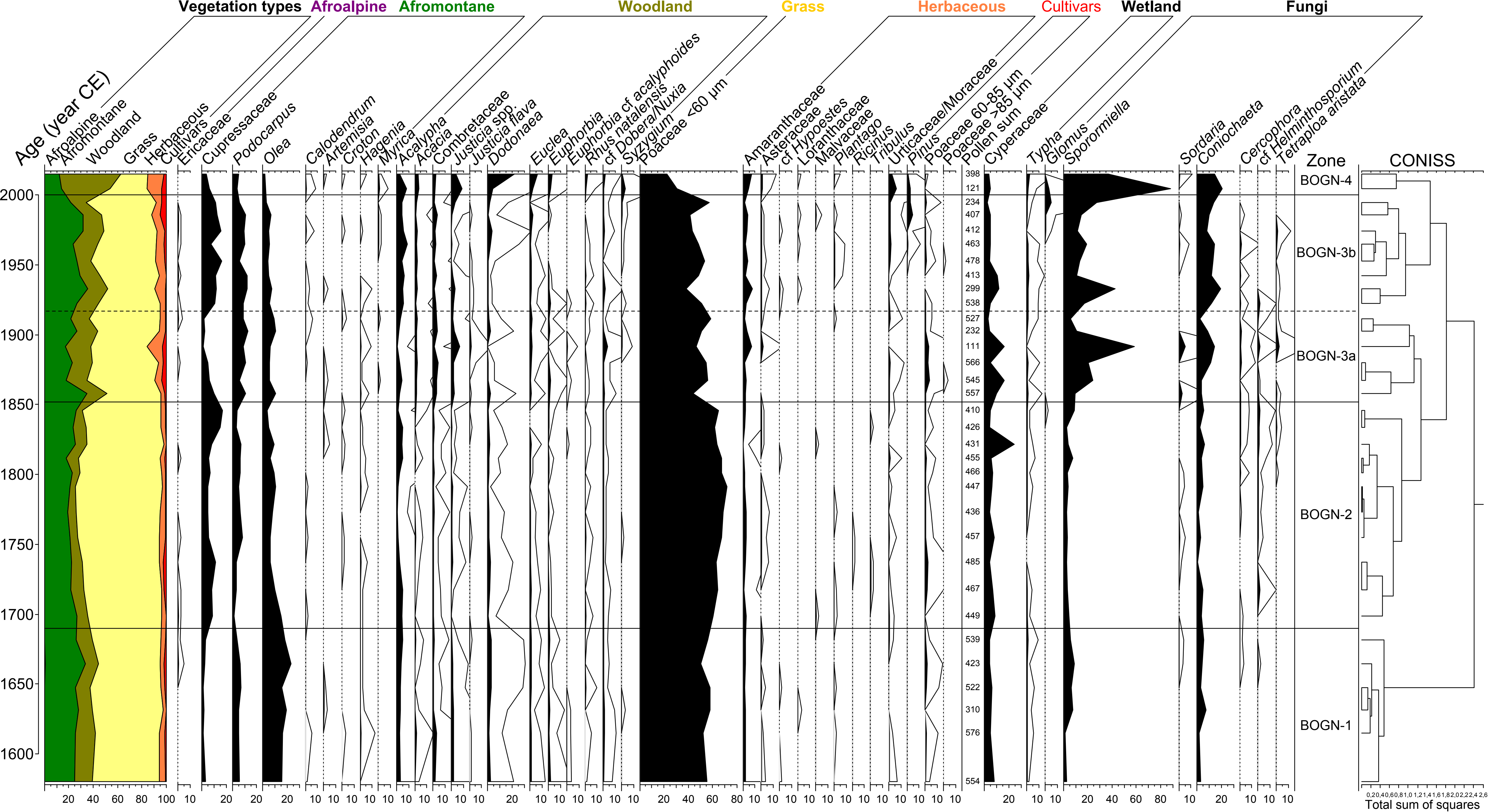












Age (year CE)

600 800 1000 1200 1400 1600 1800 2000

**a**  $^{210}\text{Pb}$   
( $\text{Bq}\cdot\text{kg}^{-1}$ )

0 200 400

$^{137}\text{Cs}$   
( $\text{Bq}\cdot\text{kg}^{-1}$ )

0 5 10

--- 1964 CE ---

